Biopolymers for Medicine

Delivering Targeted Solutions
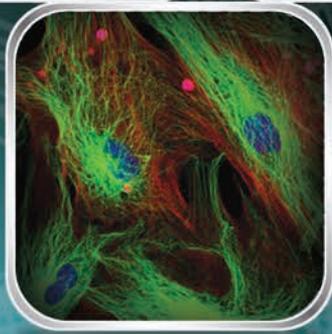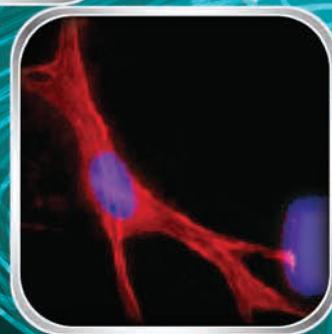
SIGMA-ALDRICH®

Introduction

Welcome to the third issue of *Material Matters*™ for 2016, focused on biocompatible and biodegradeable polymers for biomedical research. This issue highlights new material advances to deliver the promise of nanomedicine and tissue engineering through the use of innovative materials as a critical foundation to therapeutics.

In the first article, Professor Richard Hoogenboom (Ghent University, Belgium) discusses poly(2-alkyl/aryl-2-oxazoline) (PAOxs) as the next generation of biopolymers for biomedical and drug delivery applications. PAOxs, a polyethylene glycol (PEG) alternative, provide higher stability, tunability, and functionalization than PEGs, but retain the same beneficial features, such as biocompatibility, stealth behavior, and low polydispersity. The properties of PAOxs enable their use in a wide variety of biomedical applications, from targeted drug delivery to tissue engineering.

New biomaterials are often unable to successfully mimic the mechanical properties of native tissue despite extensive efforts by biopolymer researchers. In the second article, Professor Yadong Wang (University of Pittsburgh, USA) and Dr. Jeremy Harris (The Secant Group) et al. highlight a new biodegradable elastomer, poly(glycerlol sebacate), or PGS, developed in the Langer lab at MIT, for biomedical applications. PGS has many unique properties that make it well-suited for implantable applications in tissue engineering.

In the third article, David Brown (Mycodev Group, Inc.), Keith Brunt (Dalhousie School of Medicine) and Nils Rehmann (NiRem Consulting), all of Canada, highlight the unique inherent characteristics that make chitosan an excellent natural polymer for use in targeted drug delivery and discuss the advantages of chitosan derived from non-animal sources. In addition, the use of chitosan for the delivery of chemotherapeutic agents is presented.

Polyethylene glycol (PEG), is frequently used for PEGylation of peptides, proteins, siRNA, and modification of other small molecules, and for preparation of drug delivery systems such as nanoparticles. In the final article, Dr. Hui Zhu (JenKem, China) reviews several applications of Y-shape PEG derivatives in the biopharmaceutical area, including applications for PEGylation of cancer therapeutics, cocaine esterase, antibiotics, and antivirals.

In this issue, each article is accompanied by a list of polymers and related products available from Aldrich® Materials Science. For additional product information, visit us at **aldrich.com/matsci**. As always, please bother us with your new product suggestions as well as thoughts and comments for *Material Matters*™ at **matsci@sial.com** to help us continue to grow our polymer offering.

About Our Cover

Advances in nanomedicine and tissue engineering are dependent on new polymer materials to deliver the drug to the right place or to enable cell encapsulation and delivery. Innovative polymer materials provide a foundation for the creation of new scaffolds and delivery platforms that expand the possibilities of nanomedicine and tissue regeneration. In this issue, our cover art depicts several applications in which polymers act as delivery agents, from circulating polymeric nanoparticles to biomimetic hydrogels.

Table of Contents

Articles

Featured Products

Your Materials Matter

Bryce P. Nelson, Ph.D.
Materials Science Initiative Lead

*We welcome fresh product ideas. Do you have a material or compound you wish to see featured in our Materials Science line? If it is needed to accelerate your research, it matters. Send your suggestion to **matsci@sial.com** for consideration.*

Professor Scott Grayson at Tulane University (USA) kindly suggested that we offer a diverse set of high quality multi-arm poly(ethelyne glycol)s (PEGs) with a variety of terminal functionalities. These functionalized PEGs can be used as crosslinkers for PEG hydrogels and to form microspheres for biomedical applications. We have included a diverse array of functionalized PEGs near the end of the review by Dr. Hui Zhu (see page 93). In addition, we have added a number of norbornene-terminated multi-arm PEGs to our product portfolio for biomedical applications. Multi-arm PEG-norbornenes can be crosslinked into hydrogels using thiol-ene chemistry.[1] Thiol-ene photopolymerization has been used to fabricate spatially controlled hydrogels for cell encapsulation,[2] protein delivery,[3,4] and micropatterning of 3D microenvironments.[5] Furthermore, due to the tremendous control over crosslinking, hydrogels can be formed with different elasticities to investigate substrate stiffness and cell response.[6,7]

References

(1) Fairbanks, B. D. et al. *Advanced Materials* **2009**, *21*(48), 5005–5010.
(2) Anderson, et al. *Biomaterials* **2011**, *32*(14), 3564–3574.
(3) Aimetti, A. A.; Machen, A. J.; Anseth, K. S. *Biomaterials* **2009**, *30*(30), 6048–6054.
(4) Van Hove, A. H.; G. Beltejar, M. J.; Bnoit, D. S. W. *Biomaterials* **2014**, *35*(36), 9719–9730.
(5) Hynes, W. F. et al. *Biosensors* **2014**, (1), 28–44.
(6) Tokuda, E. Y.; Leight, J. L.; Anseth, K. S. *Biomaterials* **2014**, *35*(14), 4310–4318.
(7) Gould, S. T. *Biomaterials* **2014**, *35*(11), 3596–3606.

4-arm Poly(ethylene glycol) norbornene terminated

[1191287-92-9]
$[C_8H_9O_2(C_2H_4O)_nCH_2]_4C$
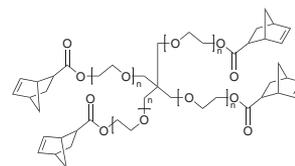
powder

PEG-norbornene; PEG-nb

▶ average M_n 10,000
mp . . . . 43 to 48 °C

store at −20 °C

808474-1G	1 g

▶ average M_n 20,000
mp . . . . 49 to 54 °C

store at −20 °C

808466-1G	1 g

POLY(2-OXAZOLINE)S:

THE VERSATILE POLYMER PLATFORM FOR BIOMEDICINE

Victor R. de la Rosa,[1] An Van Den Bulcke,[2] and Richard Hoogenboom[1]*
[1]Supramolecular Chemistry Group, Department of Organic and Macromolecular Chemistry
Ghent University, Krijgslaan 281-S4, 9000 Ghent, Belgium
[2]ChemTech, Department of Organic and Macromolecular Chemistry, Ghent University
Krijgslaan 281-S4, 9000 Ghent, Belgium
*Email: Richard.Hoogenboom@ugent.be

Introduction

The introduction of polymers into the biomedical field has opened new avenues in tissue engineering, implant design, biosensing, and drug delivery. The synergetic combination of polymers and pharmaceuticals provides a means to address significant unmet medical needs such as continuous sustained drug release, or delivery of high drug payloads to specific tissues. Thus, polymers are a key component in areas such as cancer treatment, regenerative medicine, and gene therapy.

Poly(ethylene glycol), or PEG, also known as poly(ethylene oxide), or PEO, is the most extensively used polymer in biomedicine to increase the half-life and immunogenicity of proteins. Although PEG remains the gold standard in polymer-based biomedical applications based on its low dispersity (Đ), biocompatibility, and limited recognition by the immune system (stealth behavior), it has some drawbacks and limitations. For example, anti-PEG antibodies have been observed in a significant number of patients,[1,2] including 25% of patients never treated with PEG drugs (due to its ubiquity in cosmetics and food additives). This suggests the cause of the accelerated blood clearance of PEG conjugates after multiple injections.[3] In addition, the polyether backbone of PEG is prone to oxidative degradation,[4] a significant drawback for long-term applications such as antifouling surfaces for implants[5] and probable induction of PEG-mediated complement activation.[6–8]

Nevertheless, the success of PEG in biomedical applications has paved the way for the development of the next generation of polymeric biomaterials, with greater versatility and more diverse architectural possibilities to meet the new challenges in medicine and the requirements in drug loading, responsiveness, targeting and labeling.[9–11]

Poly(2-alkyl/aryl-2-oxazoline)s, commonly abbreviated as PAOx, POx, or POZ, provide higher stability, tunability, and functionalization than PEG, while retaining the requisite features of biocompatibility,[12] stealth behavior, and low dispersity. The excellent properties of PAOx polymers enable their use in a wide variety of different biomedical applications, from targeted drug delivery and drug formulation to tissue engineering and tissue adhesives. In particular, the extraordinary synthetic versatility of PAOx allows the construction of complex polymeric architectures with finely tunable physical properties in a defined manner, making it an attractive platform for developing new approaches in precision medicine.[13,14] This overview on biomedical applications of PAOx presents a special emphasis on their contribution and potential impact on drug delivery applications.

Properties and Biocompatibility

As shown in **Figure 1**, PAOx are readily obtained via cationic ring-opening polymerization (CROP) of 2-oxazolines, resulting in polymers with a backbone composed of tertiary amides that suppress interactions with proteins and result in significantly reduced recognition by the immune system.[15]

Functionalities can be introduced at both ends of the polymer chain by selection of the electrophilic initiator [alkyl halides, acid halides, (pluri)tosylates, (pluri)triflates, (pluri)nosylates, etc.] and nucleophilic terminating agent (amines, thiolates, carboxylates, etc.). Control of the polymer chain-end functionality allows incorporation of targeting units or radiolabels for imaging, while also enabling the use of PAOx for surface or nanoparticle modification. Moreover, the side chains are tunable by modification of the substituent of the 2-oxazoline monomer, granting control over the hydrophilic–hydrophobic balance and the lower critical solution temperature (LCST) of the polymer.[16] This side-chain tunability enables the introduction of multiple functional groups along the polymer chain and the preparation of hydrogels or highly drug-loaded delivery vehicles.

Figure 2 shows a series of PAOx with an increasing degree of hydrophobicity. While poly(2-methyl-2-oxazoline), or PMeOx, displays a higher hydrophilicity than PEG,[17] PAOx with longer alkylic side-chains exhibits a thermoresponsive behavior with transition temperatures progressively lowering with the polymer side-chain hydrophobicity. In contrast to the gold standard thermoresponsive polymer for biomedical applications, poly(N-isopropylacrylamide) (PNIPAM, LCST = 32 °C, **Prod. No. 806471**), PAOx exhibits a minimal thermal hysteresis behavior and the transition temperature can be fine-tuned by copolymerization of
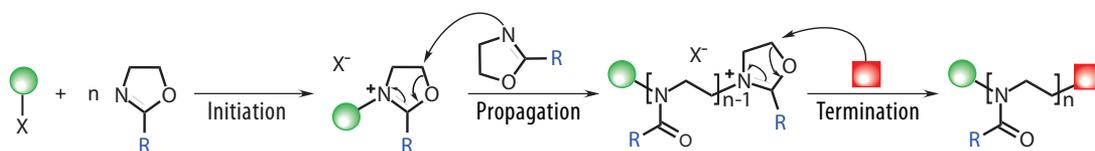

Figure 1. Living Cationic Ring-opening Polymerization (CROP) of 2-oxazolines. Both alpha and omega termini can be functionalized by the selection of initiator (tosylate in the scheme) and terminating agent (a nucleophile). Well-defined block copolymers are attainable by successive monomer addition, resulting in polymers with very low dispersity values (typically Đ = 1.05–1.30).

hydrophilic and hydrophobic 2-oxazolines.[18] This tunability makes PAOx an ideal polymer for the development of stimuli-responsive smart materials, with applications in detection, diagnostics and triggered drug delivery.[19–21]
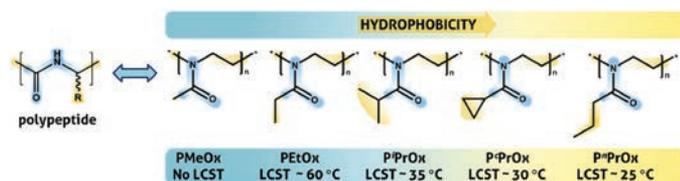

Figure 2. A series of PAOx derivatives displays the structural analogy with natural polypeptides and their amphiphilic character. The lower critical solution temperature (LCST) can be fine tuned by copolymerization. P*i*PrOx and P*n*PrOx are structural isomers and potential alternatives of poly(*N*-isopropylacrylamide) (PNIPAM, LCST = 32 °C). Adapted with permission from Reference 14.

The structural similarity of PAOx with natural polypeptides as shown in **Figure 2** accounts for their stealth behavior and excellent biocompatibility. PAOx exhibit a very fast blood clearance and remarkably low uptake in organs of the reticuloendotheliary system, as demonstrated in biodistribution studies with radio-labeled 5 kDa PMeOx and poly(2-ethyl-2-oxazoline), or PEtOx,[22] that show an apparent clearance limit of 40 kDa.[23] *In vivo* toxicity has shown no adverse effects upon repeated intravenous injections (in rats) of 10 and 20 kDa PEtOx in a broad range of concentrations (500 to 2,000 mg/kg).[17] Perhaps the most reassuring instance of PAOx biocompatibility is the development of the first commercial PAOx-based pharmaceutical, which is currently undergoing first-in-human Phase I clinical trials.[24]

As a result of their excellent biocompatibility and synthetic versatility, PAOx are attracting a growing interest as a future platform of choice in drug delivery, and significant progress in this field has already been realized. Applications in development tackle current challenges in high drug loading targeted delivery, combination therapy, sustained drug release, and formulation. The main strategies investigated using PAOx in drug delivery are summarized in **Figure 3** and can be differentiated from systems where the active pharmaceutical ingredient (API) is covalently or non-covalently linked to the polymer.

Non-covalently Linked Drug Delivery

PAOx as an Excipient in Drug Formulation

Perhaps the most straightforward contribution of polymers to drug delivery is their use as excipients, where the API is dispersed together with the polymer that serves as a matrix to enhance the drug solubility profile. The search for new drug excipients is motivated by the poor water solubility properties of an estimated 90% of newly developed drugs.[25] Hot-melt extrusion (HME) or spray-drying of adequate polymers together with the API allows the formation of solid solutions in which the drug is stabilized in an amorphous form, highly increasing its solubility and bioavailability.

De Geest et al. prepared tablet formulations of metoprolol tartrate/PEtOx and fenofibrate/PEtOx via HME using *Aquazol*. For both the hydrophilic metoprolol tartrate and the hydrophobic fenofibrate, release profiles could be either accelerated or slowed down by variation of the polymer molar mass.[26] Urbanova and co-workers demonstrated similar tunability of the acetylsalicylic acid release profile in solid dispersions with PEtOx.[27] In addition, PAOx formulations have been shown to significantly enhance the stability of sensitive cannabinoids, performing remarkably better than state-of-the-art commercial polymers.[28] Recently developed methods to produce the high molar mass, low dispersity PAOx[29] required for pharmaceutical applications are expected to accelerate the use of PAOx in drug formulation.

PAOx-based Micelle Systems

Amphiphilic polymers self-assemble into micelles or polymersomes in which the morphology can be selected by tuning the polymer length and composition. Micelle systems are advantageous since they can enable high loading of drugs with poor water solubility, a challenge especially for many new cancer treatments. In addition, micelles benefit from both passive and active targeting because they tend to accumulate in cancer tissues due to the enhanced permeability and retention (EPR) effect while serving as a platform to incorporate targeting groups.

PAOx allow for highly defined polymer structure and composition enabling fine tuning of the hydrophilic–hydrophobic balance of the polymer by copolymerization and, thus, the control on micelle size and
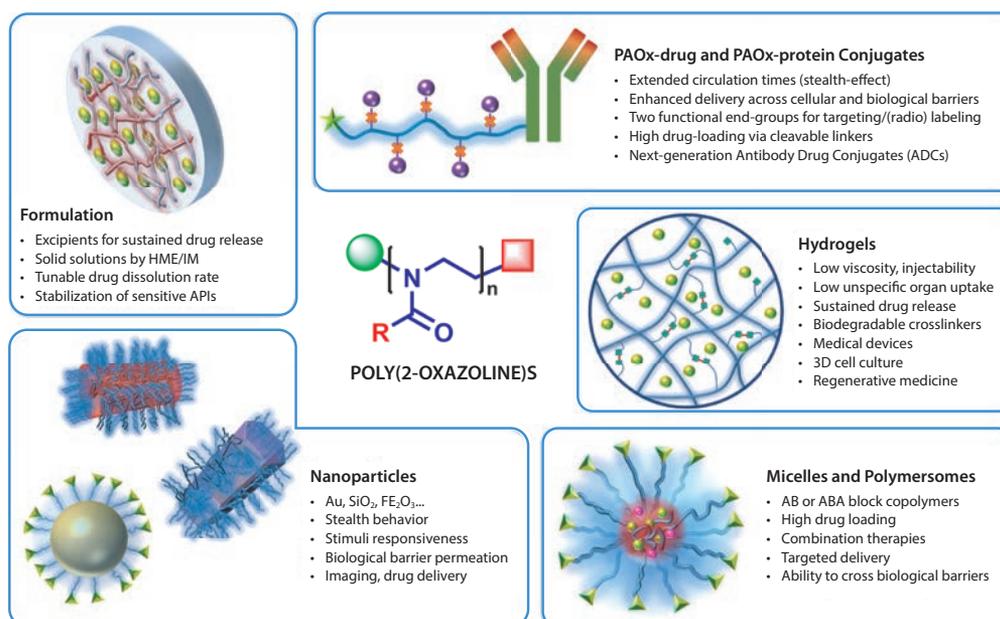


Figure 3. Overview of the main strategies that PAOx offer for drug delivery applications. The remarkable ability to tailor the material properties offered by PAOx accounts for their applicability in a diverse set of drug delivery approaches.

drug release properties. Most reported PAOx-based micellar systems feature a hybrid PAOx-polyester (PAOx-PE) diblock structure, or an ABA triblock structure synthesized by sequential addition of hydrophilic and hydrophobic 2-oxazoline monomers.

Zhao and co-workers used a Boc-NH-PEtOx-OH as a macroinitiator for the polymerization of ε-caprolactone and subsequently functionalized the hydrophilic PEtOx with a folate moiety. This resulted in folate-decorated micelles that could be loaded with doxorubicin (DOX, **Prod. No. D1515**) with capacities higher than 10 wt.%. These nanovectors showed better therapeutic efficacy and reduced toxicity than DOX when administered to nude mice bearing KB tumors.[30] A similar targeted micelle system was loaded with indocyanine green, an FDA-approved near-infrared dye, allowing both tumor imaging as well as effective photothermal therapy of KB tumors *in vivo*.[31]

Multiple targeting moieties can be incorporated in the micelle outer shell for enhanced cellular uptake by combining differently functionalized PAOx, as recently reported for a PEtOx-*b*-P(D-L-lactide) system.[32]

A very well studied micelle system developed by Kabanov, Jordan and Luxenhofer comprises an ABA triblock structure featuring a hydrophobic middle-block of poly(2-n-butyl-2-oxazoline), or PBuOx, and two outer blocks of PMeOx.[33] This polymer system yields stable micelles with sizes below 100 nm and unmatched high drug-loading capacity of anti-cancer drugs with poor water solubility. Loading capacities of up to 50 wt.% have been reported for a range of new-generation taxoids, increasing the intrinsic solubility of the APIs by up to 9,000 times.[34] Synergetic effects arising from combining multiple APIs in the micelles have also been reported for these high capacity micelle systems.[35] Currently, Kabanov's team is building a cheminformatic database to predict which drugs can best take advantage of these PAOx-based micelle carriers.

PAOx-based Hydrogels

The introduction of functionality across the polymer side-chain allows a wide variety of strategies to prepare PAOx-based hydrogels.[36,37] Lecommandoux et al. introduced reactive amine units along the PEtOx chain by partial hydrolysis. The obtained PEtOx–PEI copolymers were subsequently crosslinked with a bis-glycidyl ether in aqueous medium, resulting in biocompatible spherical nanogels with an optimal size for drug delivery applications.[38,39] Furthermore, injectable hydrogels based on PEtOx-poly(ε-caprolactone)-PEtOx have demonstrated superior biocompatibility compared to commercial Matrigel® and Pluronic® F127 (**Prod. No. P2443**) for intraocular drug delivery *in vivo*.[40]

Dargaville et al. copolymerized MeOx and 2-(dec-9-enyl)-2-oxazoline, obtaining hydrophilic polymers with alkene side-chains that were functionalized with the CRGDSG peptide sequence to promote cell adhesion. Subsequent crosslinking in the presence of a dithiol yielded transparent hydrogels in a one-pot fashion. The mild conditions of the gelation process permitted the encapsulation of fibroblast cells during the UV-mediated curing process, obtaining three-dimensional cell-polymer constructs of interest in tissue engineering and regenerative medicine.[41]

Covalently Linked Drug Conjugates

PAOx-drug and PAOx-protein Conjugation or PAOxylation

The PAOxylation of a number of proteins like trypsin, catalase, serum albumin, insulin, or uricase has yielded conjugates with performances similar to their PEGylated counterparts.[42,43] Interestingly, PEtOx-insulin conjugates were found to decrease blood glucose levels for up to 8 hours, four times longer than the free insulin.[17] Kabanov et al. functionalized a number of piperazine-terminated PAOx with an NHS-activated ester and

prepared conjugates of horseradish peroxidase.[44] The protein retained 90% of its activity, and the cellular uptake was found to increase by three to six fold compared to unmodified protein when using an amphiphilic PMeOx- or PEtOx-*b*-PBuOx copolymer. Similar copolymers were used to conjugate superoxide dismutase 1 (SOD1), showing enhanced neuronal uptake of the conjugate *in vitro* and effective passage through the blood-brain barrier *in vivo*.[45]

The introduction of clickable groups along the hydrophilic PMeOx or PEtOx chain[46] has proven to be an effective strategy for protein and drug conjugation. Copolymers of MeOx and EtOx with 2-(pent-4-ynyl)-2-oxazoline, or PynOx, provided multiple linkage points for the stabilization of virus-like particles (VLP). An icosahedral VLP was formed by supramolecular assembly of 180 copies of the coat protein of bacteriophage Qβ, and its surface was decorated with azide groups using an azido-*N*-hydroxysuccinimide ester. Following copper-catalyzed azide-alkyne cycloaddition (CuAAC) click with PMeOx/PEtOx-*ran*-PynOx copolymers resulted in PAOx-wrapped VLPs with remarkably high thermal stability. Furthermore, the particle size could be controlled by the polymer length and attachment density.[47]

Serina Therapeutics has used similar PEtOx-*ran*-PynOx polymers to create a one-week long sustained release of rotigotine for the treatment of Parkinson's disease. The API is linked to the polymer via CuAAC click chemistry using a biodegradable ester spacer, enabling sustained drug release that leads to constant plasma levels.[48] This polymer, named SER-214, is currently undergoing Phase I clinical trials and, if successful, will become the first FDA-approved PAOx therapeutic.[24]

Hoogenboom et al. introduced methyl ester functionalities across the polyoxazoline chain by copolymerization of EtOx with 2-methoxycarbonylethyl-2-oxazoline (MestOx).[49] The authors demonstrated that the resulting methyl ester functionalities decorating the polyoxazoline chain constitute a highly versatile reactive handle, as a wide variety of moieties can be introduced by direct amidation with amines. This synthetic approach further expands the PAOx toolbox for the preparation of novel PAOx-drug conjugates.[50]

Future multiple drug-loaded PAOx-API conjugates will most definitely be improved by the addition of targeting moieties in the polymer chain-ends, such as folate groups or antibodies. There is, thus, ample room for advances in this fascinating field.

PAOx-functionalized Nanoparticles

Nanoparticles (NPs) are able to accommodate multiple functional groups while providing unique optical, electronic, or magnetic properties and, therefore, have enormous potential in biomedical sciences, including imaging and drug delivery. When connected to NPs, PAOx form a stealth corona that provides nanoparticle stabilization, prevents rapid clearance, and serves as a reliable scaffold for the incorporation of bioactive compounds. In this context, Benetti and co-workers functionalized PMeOx-OH with nitrodopamine for the functionalization of ZnO nanocrystals of interest for imaging. Functionalization with 4 kDa PMeOx yielded individually dispersed nanocrystals with an outstanding stability of up to 9 months.[51]

In addition to granting stability and stealth effect to NPs, PAOx thermo-responsive properties have been exploited to prepare responsive or *smart* NPs that aggregate upon the application of external stimuli.[20] Recently, fluorescent NPs based on a polyorganosiloxane were functionalized with the thermo-responsive poly(2-isopropyl-2-oxazoline), or P^{i}PrOx, (**Figure 2**). Below 31 °C, the P^{i}PrOx nanoparticles exhibit an anti-fouling behavior when dispersed in a serum-containing medium. However, heating beyond this temperature triggers the adsorption of serum proteins on the nanoparticles, reversible by lowering the temperature. This strategy could be applied to increase nanoparticle agglomeration in the targeted cells or organs by applying local heating.[19]

For questions, product data, or new product suggestions, contact us at **matsci@sial.com**.

77

Finally, as seen before for PAOx-based micelles and conjugates, PAOx can enhance nanoparticle permeation through biological barriers. Khutoryanskiy et al. used 5 kDa alkyne-terminated PEtOx to functionalize thiolated silica NPs via thiol-ene chemistry. The resulting NPs exhibited enhanced permeation through porcine gastric mucosa *ex vivo* in a similar way as analogous PEGylated NPs.[52] Considering the straightforward tunability of PAOx composition and hydrophilic–hydrophobic balance, further developments are expected to bring even more efficient drug delivery vehicles with improved ability to permeate biological barriers.

Conclusions and Outlook

The large number of possibilities offered by polyoxazolines for creating materials that impact a broad variety of biomedical applications is unique for this polymer class. PAOx have already demonstrated excellent biocompatibility and stability in a large number of independent studies, and the first in-human Phase I clinical trials of a polyoxazoline therapeutical are ongoing. By virtue of their structural and functional diversity, and the high control and definition that the polymerization of oxazolines offers, PAOx constitute a very attractive and versatile platform for the development of next-generation drug delivery systems.

Acknowledgments

References

(1) Armstrong, J. K.; Hempel, G.; Koling, S.; Chan, L. S.; Fisher, T.; Meiselman, H. J.; Garratty, G. *Cancer* **2007**, *110*, 103.
(2) Tagami, T.; Nakamura, K.; Shimizu, T.; Yamazaki, N.; Ishida, T.; Kiwada, H. *J. Control. Release* **2010**, *142*, 160.
(3) Suzuki, T.; Ichihara, M.; Hyodo, K.; Yamamoto, E.; Ishida, T.; Kiwada, H.; Ishihara, H.; Kikuchi, H. *Int. J. Pharm.* **2012**, *436*, 636.
(4) Ostuni, E.; Chapman, R. G.; Holmlin, R. E.; Takayama, S.; Whitesides, G. M. *Langmuir* **2001**, *17*, 5605.
(5) Arima, Y.; Toda, M.; Iwata, H. *Biomaterials* **2008**, *29*, 551.
(6) He, Z.; Liu, J.; Du, L. *Nanoscale* **2014**, *6*, 9017.
(7) Knop, K.; Hoogenboom, R.; Fischer, D.; Schubert, U. S. *Angew. Chem. Int. Ed.* **2010**, *49*, 6288.
(8) Barz, M.; Luxenhofer, R.; Zentel, R.; Vicent, M. J. *Polym. Chem.* **2011**, *2*, 1900.
(9) Fleige, E.; Quadir, M. A.; Haag, R. *Adv. Drug Delivery Rev.* **2012**, *64*, 866.
(10) Lee, J. S.; Feijen, J. *J. Control. Release* **2012**, *161*, 473.
(11) Duncan, R.; Vicent, M. J. *J. Adv. Drug Delivery Rev.* **2013**, *65*, 60.
(12) Bauer, M.; Lautenschlaeger, C.; Kempe, K.; Tauhardt, L.; Schubert, U. S.; Fischer, D. *Macromol. Biosci.* **2012**, *12*, 986.
(13) Schlaad, H.; Hoogenboom, R. *Macromol. Rapid Commun.* **2012**, *33*, 1593.
(14) de la Rosa, V. R. *J. Mater. Sci.: Mater. Med.* **2014**, *25*, 1211.
(15) Chapman, R. G.; Ostuni, E.; Takayama, S.; Holmlin, R. E.; Yan, L.; Whitesides, G. M. *J. Am. Chem. Soc.* **2000**, *122*, 8303.
(16) Verbraeken, B.; Lava, K.; Hoogenboom, R. In *Encyclopedia of Polymer Science and Technology*; John Wiley & Sons, Inc.: **2014**, p 1.
(17) Viegas, T. X.; Bentley, M. D.; Harris, J. M.; Fang, Z.; Yoon, K.; Dizman, B.; Weimer, R.; Mero, A.; Pasut, G.; Veronese, F. M. *Bioconjugate Chem.* **2011**, *22*, 976.
(18) Hoogenboom, R.; Thijs, H. M. L.; Jochems, M. J. H. C.; van Lankvelt, B. M.; Fijten, M. W. M.; Schubert, U. S. *Chem. Commun.* **2008**, 5758.
(19) Koshkina, O.; Lang, T.; Thiermann, R.; Docter, D.; Stauber, R. H.; Secker, C.; Schlaad, H.; Weidner, S.; Mohr, B.; Maskos, M.; Bertin, A. *Langmuir* **2015**, *31*, 8873.
(20) de la Rosa, V. R.; Zhang, Z.; De Geest, B. G.; Hoogenboom, R. *Adv. Funct. Mater.* **2015**, *25*, 2511.
(21) Weber, C.; Hoogenboom, R.; Schubert, U. S. *Prog. Polym. Sci.* **2012**, *37*, 686.
(22) Gaertner, F. C.; Luxenhofer, R.; Blechert, B.; Jordan, R.; Essler, M. *J. Control. Release* **2007**, *119*, 291.
(23) Wyffels, L.; Verbrugghen, T.; Monnery, B. D.; Glassner, M.; Stroobants, S.; Hoogenboom, R.; Staelens, S. *J. Control. Release* **2016**, *235*, 63.
(24) Serina Therapeutics. http://www.serinatherapeutics.com (accessed June 10, 2016).
(25) *Formulating Poorly Water Soluble Drugs*; Williams III, R. O.; Watts, A. B.; Miller, D. A., Eds.; Springer, **2012**; Vol. 3.
(26) Claeys, B.; Vervaeck, A.; Vervaet, C.; Remon, J. P.; Hoogenboom, R.; De Geest, B. G. *Macromol. Rapid Commun.* **2012**, *33*, 1701.
(27) Policianova, O.; Brus, J.; Hruby, M.; Urbanova, M. *Pharm. Dev. Technol.* **2015**, *20*, 935.
(28) Bender, J. C. M. E.; Hoogenboom, R.; Van Vliet, P. A. A.; Bender Analytical Holding B.V. *Drug delivery system comprising polyoxazoline and a bioactive agent.* World Patent WO2011002285 A1, 2011.
(29) Monnery, B. D.; Shaunak, S.; Thanou, M.; Steinke, J. H. G. *Macromolecules* **2015**, *48*, 3197.
(30) Qiu, L.-Y.; Yan, L.; Zhang, L.; Jin, Y.-M.; Zhao, Q.-H. *Int. J. Pharm.* **2013**, *456*, 315.
(31) Yan, L.; Qiu, L. *Nanomedicine* **2015**, *10*, 361.
(32) Gao, Y.; Zhang, C.; Zhou, Y.; Li, J.; Zhao, L.; Li, Y.; Liu, Y.; Li, X. *Pharm. Res.* **2015**, *32*, 2649.
(33) Luxenhofer, R.; Schulz, A.; Roques, C.; Li, S.; Bronich, T. K.; Batrakova, E. V.; Jordan, R.; Kabanov, A. V. *Biomaterials* **2010**, *31*, 4972.
(34) He, Z.; Schulz, A.; Wan, X.; Seitz, J.; Bludau, H.; Alakhova, D. Y.; Darr, D. B.; Perou, C. M.; Jordan, R.; Ojima, I.; Kabanov, A. V.; Luxenhofer, R. *J. Control. Release* **2015**, *208*, 67.
(35) Han, Y.; He, Z.; Schulz, A.; Bronich, T. K.; Jordan, R.; Luxenhofer, R.; Kabanov, A. V. *Mol. Pharm.* **2012**, *9*, 2302.
(36) Hartlieb, M.; Kempe, K.; Schubert, U. S. *J. Mater. Chem. B* **2015**, *3*, 526.
(37) Kelly, A. M.; Wiesbrock, F. *Macromol. Rapid Commun.* **2012**, *33*, 1632.
(38) Legros, C.; Wirotius, A.-L.; De Pauw-Gillet, M.-C.; Tam, K. C.; Taton, D.; Lecommandoux, S. *Biomacromolecules* **2015**, *16*, 183.
(39) Legros, C.; De Pauw-Gillet, M.-C.; Tam, K. C.; Lecommmandoux, S.; Taton, D. *Polym. Chem.* **2013**, *4*, 4801.
(40) Hwang, Y.-S.; Chiang, P.-R.; Hong, W.-H.; Chiao, C.-C.; Chu, I. M.; Hsiue, G.-H.; Shen, C.-R. *PLoS One* **2013**, *8*, e67495.
(41) Farrugia, B. L.; Kempe, K.; Schubert, U. S.; Hoogenboom, R.; Dargaville, T. R. *Biomacromolecules* **2013**, *14*, 2724.
(42) Mero, A.; Fang, Z.; Pasut, G.; Veronese, F. M.; Viegas, T. X. *J. Control. Release* **2012**, *159*, 353.
(43) Mero, A.; Pasut, G.; Via, L. D.; Fijten, M. W. M.; Schubert, U. S.; Hoogenboom, R.; Veronese, F. M. *J. Control. Release* **2008**, *125*, 87.
(44) Tong, J.; Luxenhofer, R.; Yi, X.; Jordan, R.; Kabanov, A. V. *Mol. Pharm.* **2010**, *7*, 984.
(45) Tong, J.; Yi, X.; Luxenhofer, R.; Banks, W. A.; Jordan, R.; Zimmerman, M. C.; Kabanov, A. V. *Mol. Pharm.* **2013**, *10*, 360.
(46) Lava, K.; Verbraeken, B.; Hoogenboom, R. *Eur. Polym. J.* **2015**, *65*, 98.
(47) Manzenrieder, F.; Luxenhofer, R.; Retzlaff, M.; Jordan, R.; Finn, M. G. *Angew. Chem. Int. Ed.* **2011**, *50*, 2601.
(48) Eskow Jaunarajs, K. L.; Standaert, D. G.; Viegas, T. X.; Bentley, M. D.; Fang, Z.; Dizman, B.; Yoon, K.; Weimer, R.; Ravenscroft, P.; Johnston, T. H.; Hill, M. P.; Brotchie, J. M.; Moreadith, R. W. *Movement Disorders* **2013**, *28*, 1675.
(49) Bouten, P. J. M.; Hertsen, D.; Vergaelen, M.; Monnery, B. D.; Boerman, M. A.; Goossens, H.; Catak, S.; van Hest, J. C. M.; Van Speybroeck, V.; Hoogenboom, R. *Polym. Chem.* **2015**, *6*, 514.
(50) Mees, M. A.; Hoogenboom, R. *Macromolecules* **2015**, *48*, 3531.
(51) Morgese, G.; Causin, V.; Maggini, M.; Corrà, S.; Gross, S.; Benetti, E. M. *Chem. Mater.* **2015**, *27*, 2957.
(52) Caló, E.; Khutoryanskiy, V. V. *Eur. Polym. J.* **2015**, *65*, 252.

Poly(oxazoline)s

For a complete list of available materials, visit aldrich.com/pox.

Low PDI Poly(oxazoline)s

Name	Structure	Molecular Weight (Avg M_n)	PDI	Prod. No.
Poly(2-ethyl-2-oxazoline)		5,000	≤1.2	740713-5G
		10,000	<1.3	741906-5G
		25,000	≤1.4	741884-5G
Ultroxa®: Poly(2-ethyl-2-oxazoline)		50,000	≤1.25	900353-1G

n = 500

Name	Structure	Molecular Weight (Avg M_n)	PDI	Prod. No.
Ultroxa®: Poly(2-methyl-2-oxazoline)	n = 118	10,000	≤1.2	900350-1G
Ultroxa®: Poly(2-propyl-2-oxazoline)	n = 89	10,000	≤1.2	900352-1G
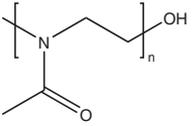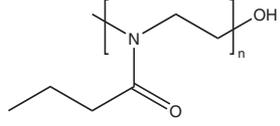
High M_w Poly(2-ethyl-2-oxazoline)s
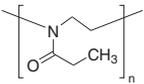
Name	Structure	Molecular Weight (Avg M_w)	PDI	Prod. No.
Poly(2-ethyl-2-oxazoline)		~50,000	3-4	372846-100G 372846-500G
		~200,000	3-4	372854-100G
		~500,000	3-4	373974-100G 373974-500G

Functionalized Poly(oxazoline)s

Name	Structure	Molecular Weight (Avg M_n)	PDI	Prod. No.
Poly(2-ethyl-2-oxazoline), alkyne terminated		5,000	≤1.2	778338-1G
		2,000	≤1.1	747262-1G
Poly(2-ethyl-2-oxazoline), α-benzyl, ω-thiol terminated		2,000	<1.3	809438-5G
		10,000	<1.3	809446-5G
		5,000	<1.3	900265-5G
Poly(2-methyl-2-oxazoline), α-benzyl, ω-azide terminated		2,000	<1.3	778303-1G
		5,000	<1.3	778311-1G
Poly(2-methyl-2-oxazoline), hydroxy terminated		2,000	<1.2	795275-5G
		5,000	<1.3	795283-5G
Ultroxa®: Poly(2-ethyl-2-oxazoline)	n = 500	5,000	≤1.15	900360-500MG
		10,000	≤1.2	900359-500MG
		10,000	≤1.2	900357-500MG
		10,000	≤1.2	900355-500MG
Ultroxa®: Poly(2-methyl-2-oxazoline)	n = 118	10,000	≤1.2	900354-500MG
		10,000	≤1.2	900358-500MG
Ultroxa®: Poly(2-propyl-2-oxazoline)	n = 89	10,000	≤1.2	900356-500MG
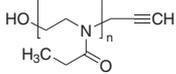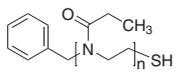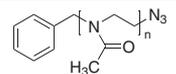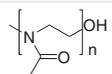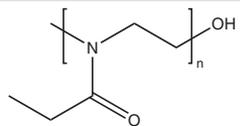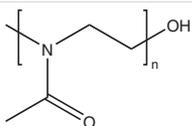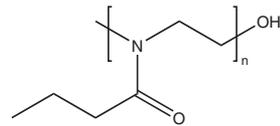
For questions, product data, or new product suggestions, contact us at matsci@sial.com.

79

POLY(GLYCEROL SEBACATE)
IN TISSUE ENGINEERING AND REGENERATIVE MEDICINE

Yadong Wang,[1] Steven Lu,[2] Peter Gabriele,[2] Jeremy J. Harris[2]*
[1]Department of Bioengineering, University of Pittsburgh, Pittsburgh, PA 15261 USA
[2]Research and Development, The Secant Group, LLC, Telford, PA 18969 USA
*Email: Jeremy.Harris@secant.com

Introduction

The world of commercial biomaterials has stagnated over the past 30 years as few materials have successfully transitioned from the bench to clinical use. Synthetic aliphatic polyesters have continued to dominate the field of resorbable biomaterials due to their long history and track record of approval with the U.S. Food and Drug Administration (FDA). Despite a plethora of research to develop biocompatible, biodegradable polymers, new biomaterials have suffered from compliance mismatch, i.e., the failure to successfully mimic the mechanical properties of natural tissue. To address these concerns, poly(glycerol sebacate) (PGS) was developed in the lab of Professor Robert Langer as a tough, biodegradable elastomer.[1] Since this discovery, the biomedical engineering community has used PGS in a multitude of implantable applications in the areas of cardiovascular, neurovascular, orthopedic, and soft tissue.[2]

PGS is a simple glycerol-ester polymer created from the basic mammalian metabolites of glycerol and sebacic acid, both of which have a regulatory background with the FDA.[1] Originally designed as a biodegradable polymer with improved elastic mechanical properties and biocompatibility, research on PGS-based medical applications has uncovered a number of unique properties that have bolstered its utility as a biomaterial. In addition to its elasticity, PGS demonstrates minimal swelling, undergoes surface degradation and exhibits mild acute and chronic inflammatory responses *in vivo*. Although the majority of researchers use the thermoset elastomer form of PGS, the polymer is customizable through a continuum of resin forms. Depending on the degree of polymerization, PGS can be manufactured as a soft gel, a lubricious Vaseline®-like paste, a thermoplastic, or a thermoset depending on the applications. Through manipulation of the various morphologies, PGS can also be formulated as a coating for a range of medical implants and extruded into luminal structures, sheets, rods, and other geometric shapes. Furthermore, the polymer is compatible with a host of biologic materials such as collagen, bone minerals and extracellular matrix (ECM)-like compositions, further making it an ideal bioresorbable material for tissue engineering, regenerative medicine applications, and the biomedical device industry.

Poly(glycerol Sebacate)

Design and Structure

Current interest in bioelastomers for tissue engineering is largely driven by the need for soft-tissue repair. PGS was created specifically for engineering soft tissues in dynamic mechanical environments such as the cardiovascular system.[1] Made from glycerol and sebacic acid via polycondensation, the ester bonds in the polymer backbone covalently crosslink to form a three-dimensional (3D) network of random coils, which resembles the structure of vulcanized rubber and gives rise to rubber-like elasticity (**Figure 1**). Hydrogen bonding interactions between hydroxyl groups further enhance the mechanical properties of PGS. Due to the ester linkages, both the polymer backbone and crosslinks can undergo hydrolytic degradation.
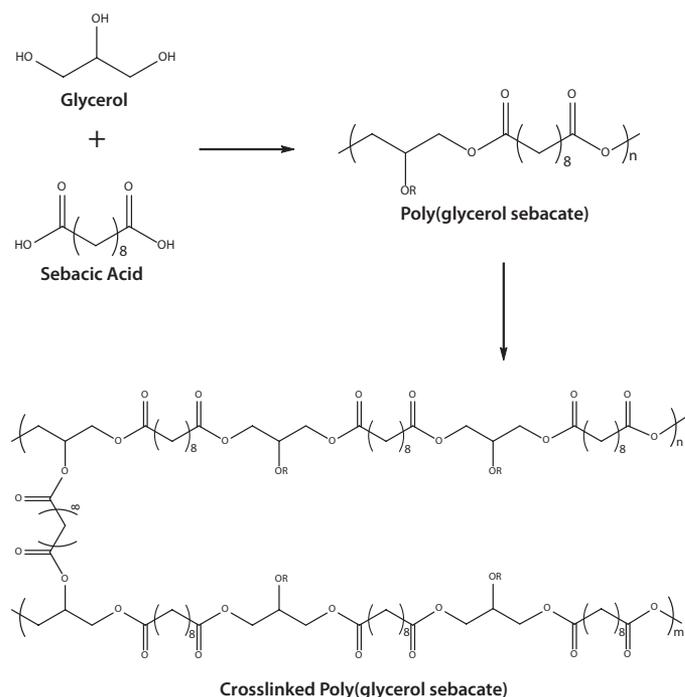

Figure 1. Reaction schematic for poly(glycerol sebacate). PGS is synthesized from glycerol and sebacic acid and further curing under heat and vacuum to produce a crosslinked PGS thermoset.

Synthesis and Mechanical Properties

PGS is synthesized via a polycondensation reaction between glycerol and sebacic acid to first form a pre-polymer resin which is then converted into the thermoset elastomer. In particular, both starting materials are inexpensive and can be obtained from renewable resources; sebacic acid for example, is derived from castor oil.[3] The synthesis of PGS also utilizes an environmentally friendly chemistry without the need for toxic solvents or catalysts, resulting in a synthetic biomaterial through an overall sustainable synthesis. Several synthesis routes are reported in the literature but the most commonly used two-step method is described here. The reactor is first charged with the monomers and heated to 120 °C under a blanket of N_2. Upon forming a homogenous solution, the mixture is further heated for 24 hours. The reactor is then placed under vacuum (40 mTorr–10 Torr) for an additional 24–48 hours depending on the desired degree of polymerization. At this point, the resin or pre-polymer is complete and ready for the second step—to create the thermoset elastomer. The resin can be used neat as a casted film, molded to a specific shape, or reduced in a solvent for casting or dip-coating applications. The resin is cured for 24–96 hours depending on the desired mechanical properties required for the elastomer.

One advantage of PGS is the ability to tune its mechanical properties by making small changes to the polymerization and curing procedures. Elastomer modulus values are directly related to the degree of crosslinking and range from 0.77–1.9 MPa for 48 and 96 hour cure times, respectively. A wider window of modulus values is achieved by manipulating the monomer stoichiometry where modulus values can be tuned from 0.01–5 MPa. Altering monomer stoichiometry also allows fine tuning of both molecular weight and free chemical functionality. Average molecular weight values range from 2,000 to >200,000 Da and can be tuned simply by changing the glycerol:sebacic acid ratio. Chemical functionality (as measured by acid number titration) ranges from 110–10 mg/g, resulting in PGS with varying hydrophilicity and reactivity of the elastomer.

Degradability and Biocompatibility

PGS degrades primarily through hydrolysis of the ester linkage into smaller oligomers and ultimately to the starting monomers, glycerol and sebacic acid. PGS degradation is unique and differs from other resorbable polymers (e.g., polylactide, polyglycolide, and copolymers) in that PGS degrades via surface erosion as opposed to bulk erosion.[4] The significance of this is demonstrated in a linear degradation profile over time with a controlled loss of mechanical properties, in contrast to bulk erosion where mechanical properties exhibit a catastrophic decrease. Many studies have evaluated the *in vitro* degradation hoping to model *in vivo* performance. However, there exists a poor correlation between *in vitro* and *in vivo* degradation behavior. *In vitro* studies performed under a range of conditions typically show upwards of a 20% mass loss at 30 days compared to a 70% mass loss observed in subcutaneous tissues.[4b] Despite the accelerated degradation kinetics of PGS *in vivo* relative to *in vitro* model conditions, the degradation rate can be tuned by modulating crosslinking density via cure time and temperature.[5]

The hydrolytic degradation of PGS into its component monomers, glycerol and sebacic acid, provides a resorbable material with high biocompatibility. Glycerol is a metabolic building block for lipids and has a long history of use in pharmaceuticals. Sebacic acid is the natural metabolite intermediate in ω-oxidation of medium and long-chain fatty acids. Further, co-polymers containing sebacic acid are used in chemotherapeutic drug delivery.[6] Various studies have evaluated the biocompatibility of PGS with both *in vitro* assays and *in vivo* implantation studies. PGS has shown to be non-cytotoxic *in vitro*[1] and induces a minimal inflammatory response with little fibrous capsule formation, likely due to the surface degradation behavior of PGS.[7]

Applications in Tissue Engineering and Regenerative Medicine

Tissue engineering has advanced rapidly over the last three decades, and part of the driving force of innovation in the field comes from novel biodegradable elastomeric biomaterials.[8] All bodily tissues are inherently elastic to some degree and many implants/grafts partly fail due to a mechanical property mismatch between native and engineered constructs.[9] For materials interfacing with vascular tissue, substrate elasticity and mechanical stimulation significantly influence cell functions and tissue development.[10] Thus elastomeric materials are recognized as an important class of scaffold materials for vascular tissue and other soft tissue regenerative applications.

Applications in Cardiovascular Tissue

Mechanical properties are a particularly important criteria for the selection of materials used in cardiovascular applications. In particular, PGS shows little plastic deformation, making it attractive for engineering cardiovascular tissues. Small-diameter arterial grafts are still a major challenge in tissue engineering, and highly porous PGS scaffolds can be particularly effective in the engineering of small arteries.[11] Moreover, endothelial progenitor cells and smooth muscle cells (SMCs) adhere and proliferate well on PGS.[11d] SMCs cultured in PGS scaffolds co-express elastin and collagen, leading to highly compliant engineered blood vessels.[11c] Furthermore, while the amount of tropoelastin made by these cells is identical on PGS and PLGA scaffolds, the elastic PGS substrate allows for crosslinking of tropoelastin into desmosine-crosslinked elastin.[11b] In a rat abdominal aorta model, composite arterial grafts comprised of PGS tubes reinforced with a polycaprolactone nanofiber sheath demonstrated constructive remodeling of the graft into neoarteries within 3 months.[12] The neoartery mimicked the native artery mechanically, biochemically, and anatomically, and the neoarteries were well integrated with host vasculature. Remarkably, the neoartery pulsed synchronously with host arteries. After one year post-implant, the neoarteries contained the same amount of elastin as their native counterpart and had regenerated in the adventitia of the neoarteries (**Figure 2**).[13]
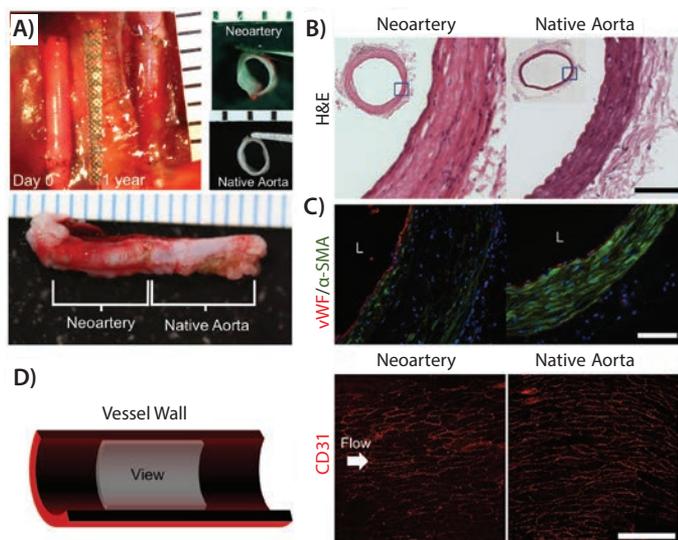
Figure 2. Gross morphology and tissue architecture of neoarteries resemble native arteries. **A)** Top left: transformation of graft into neoartery *in situ* over the course of 1 year. Nondegradable sutures (black) mark the graft location. Top right: Transverse view of explanted neoarteries resembles that of native aortas. Bottom: Longitudinal view of explanted neoarteries resembles the adjacent native aorta. All ruler ticks are 1 mm. **B)** H&E stained transverse sections of the middle of neoarteries show similar tissue architecture with native aortas, with no visible graft material residues. Scale bar 100 mm. **C)** Neoartery sections immunostained for von Willebrand factor (vWF, red) and α-smooth muscle actin (α-SMA, green). The luminal surface of neoarteries is completely covered by vWF positive cells (red), suggesting a confluent endothelium. Neoarteries contain a media-like middle layer of the vascular wall rich in α-SMA positive cells with circumferentially elongated nuclei, similar to vascular smooth muscle found in native aortas. The outermost layer of neoarteries lacks α-SMA, resembling native adventitia. Some cells in the media-like layer are negative for α-SMA, and some cells adjacent to the endothelium are α-SMA positive but not circumferentially elongated. L indicates vessel lumen. Nuclei stained with DAPI (blue). **D)** *En face* view of the luminal surface of neoarteries shows complete coverage by CD31 positive cells with cobblestone-like morphology and alignment parallel to the direction of blood flow, an arrangement similar to that found in native aortas. Neoarteries were cut open longitudinally and imaged as whole mounts using confocal microscopy and z-stack flattening. Arrow indicates the direction of blood flow. Scale bar 100 mm. Reprinted by permission from Reference 13. Copyright 2013, Elsevier Ltd.

PGS is also used extensively in cardiac tissue engineering[14] due to the ease in modulating the mechanical properties of PGS to readily match those of myocardial tissues.[5] In one application, PGS was used to fabricate highly porous scaffolds with parallel channels that mimic the capillary networks found in native myocardium.[14c] Co-cultures of cardiac fibroblasts and cardiomyocytes in a perfusion bioreactor with oxygen carriers yielded contractile constructs within 11 days.[14d] When placed *in vivo*, cell-free PGS scaffolds vascularize after implantation in an infarcted rat myocardium model within 2 weeks.[14d] Recently, a PGS scaffold with an accordion-like honeycomb microstructure was created (**Figure 3**).[14a] Its stiffness was controlled by curing time in order to match the mechanical properties of rat right ventricular myocardium. Additionally, PGS scaffolds have been precoated with ECM proteins to provide ligands for increased cell interaction which increased cellularity, enhanced ECM protein production, and modulated the differentiation of endothelial progenitor cells.[15]

Applications in Nerve Tissue

PGS has also demonstrated promise as a scaffold material for nerve regeneration.[7] The *in vitro* and *in vivo* neural biocompatibility of PGS has been systematically evaluated. Primary Schwann cells showed similar attachment rate and metabolic activity on both PGS and PLGA surfaces *in vitro*. The cells on PGS had a higher proliferation rate and lower apoptotic activity than those on PLGA. *In vivo* implantation juxtaposed to the sciatic nerve revealed PGS causes a significantly lower chronic inflammatory response than PLGA, likely due to the minimal swelling and surface eroding characteristics of PGS. A recent study investigated microfabricated PGS porous scaffolding for retinal progenitor cell (RPC) grafting. The scaffold had a Young's modulus of 1.66 ± 0.23 MPa and a maximal strain of $113 \pm 22\%$.[16] These mechanical properties more closely resemble those of retinal tissue (Young's modulus of 0.1 MPa and maximal strain of 83%) than the traditional PLA/PLGA blend (Young's modulus of 9.0 ± 1.7 MPa and maximal strain of 9%) used for RPC delivery. The *in vitro* study revealed that RPCs adhere to and proliferate well in the PGS scaffold, and shows a trend toward differentiation. Subretinal transplantations demonstrated long-term RPC survival and high levels of RPC migration into host retinal tissue.[17]
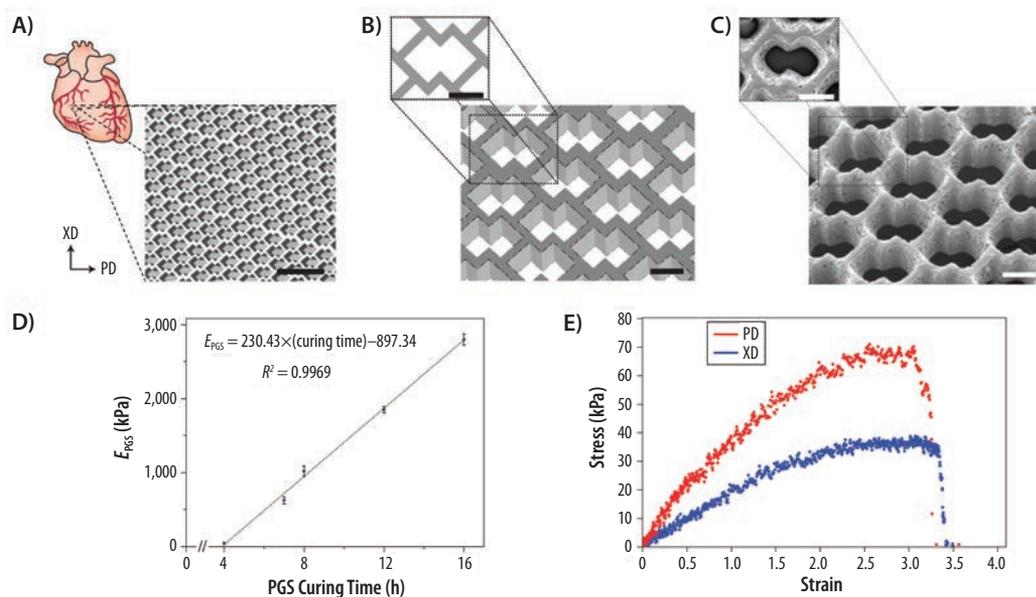
Figure 3. Accordion-like honeycomb scaffolds yield anisotropic mechanical properties similar to native myocardium. **A,B)** Schematic diagrams illustrating the accordion-like honeycomb design constructed by two overlapping 200 × 200 μm squares rotated 45° (diamonds). Preferred (PD) and orthogonal cross-preferred (XD) material directions, respectively, corresponding to circumferential and longitudinal axes of the heart, are indicated. Scale bars: 1 mm (**A**) and 200 μm (**B**). **C)** Scanning electron micrographs demonstrating the fidelity of excimer laser microablation in rendering an accordion-like honeycomb design in PGS. Scale bars: 200 μm. **D)** PGS curing time was systematically varied, yielding a linear dependence of PGS effective stiffness (E_{PGS}) on curing time within the tested range. **E)** Representative uniaxial stress–strain plots for accordion-like honeycomb scaffolds with cultured neonatal rat heart cells (scaffolds were fabricated from PGS membranes cured for 7.5 h at 160 °C; neonatal rat heart cells were cultured for 1 week). Reprinted by permission from Reference 19. Copyright 2008, Nature Publishing Group.

Applications in Bone Tissue

Although bone is a hard tissue, it develops from soft collagenous tissue in the embryonic stage. Similarly, the natural bone healing process also starts from a soft provisional tissue called the callus. For this reason, scaffolds made from PGS elastomer were used to heal a non-union bony defect. To do this, a porous PGS tube was used to join two ends of a completely transected ulna in a rabbit model.[18] Healing started with the formation of a cartilage tissue similar to a callus, which progressively mineralized and completely bridged the defect within 2 months as examined by micro-CT. Results revealed the lower stiffness PGS elastomer can create a load-transducing environment in which bone regeneration more effectively occurs. In contrast, metallic implants can cause stress shielding of the bone making healing more difficult.

Coating Applications for Medical Textiles

Coating technology plays a significant role in medical device development as it provides a means of modifying the underlying substrate and enhancing the performance of the device. PGS has shown tremendous promise as a coating material; its resin is easily reducible in a wide range of solvents (e.g., ethyl acetate, THF, acetone, 1,3-dioxolane, and various alcohols) resulting in a solution that can be used in dip and spray coating applications. **Figure 4** shows a range of textile substrates (PET, polypropylene, PGA, and nitinol) coated with a smooth conformable thin film of PGS. Enhanced mechanical properties, improved biocompatibility, and antimicrobial properties are all features imparted by a PGS coating, illustrating its utility in the medical device space.
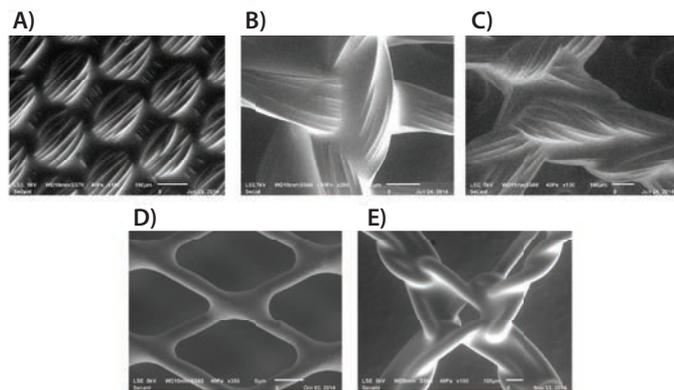
Figure 4. SEM images of Regenerez coatings deposited on a range of commonly used medical device textile components: **A)** dip-coated poly(ethylene terephthalate) woven, **B)** dip-coated poly(glycolic acid) knit, **C)** dip-coated PEEK mesh, **D)** spray-coated nitinol braid, and **E)** dip-coated poly(propylene) mesh. SEM images provided by Carissa Smoot of the Secant Group.

Conclusions

Biomaterials will continue to play an important role in medical device and regenerative medicine as a need will always exist for materials that are able to mimic the properties of native tissue. PGS has a multitude of properties which makes it an ideal material to fill the many technological demands of device and tissue engineering applications. Over the past 15 years, PGS has been utilized in applications within the fields of cardiovascular, nervous, soft, and hard tissue and continues to find new uses today such as coatings for implantable devices. Over this timeframe, PGS has progressed from the research lab to commercialization with the introduction of Regenerez® Poly(glycerol Sebacate) Resin. Recent research advances, as outlined here, will certainly expand the utility and application of this versatile biomaterial.

References

(1) Wang, Y.; Ameer, G. A.; Sheppard, B. J.; Langer, R. *Nat. Biotechnol.* **2002**, *20* (6), 602–6.

(2) Rai, R.; Tallawi, M.; Grigore, A.; Boccaccini, A. R. *Prog. Polym. Sci.* **2012**, *37* (8), 1051–1078.

(3) Chen, Q.; Liang, S.; Thouas, G. A. *Prog. Polym. Sci.* **2013**, *38* (3–4), 584–671.

(4) (a) Pomerantseva, I.; Krebs, N.; Hart, A.; Neville, C. M.; Huang, A. Y.; Sundback, C. A. *J. Biomed. Mater. Res. A* **2009**, *91* (4), 1038–47; (b) Wang, Y.; Kim, Y. M.; Langer, R. *J. Biomed. Mater. Res. A* **2003**, *66* (1), 192–7.

(5) Chen, Q. Z.; Bismarck, A.; Hansen, U.; Junaid, S.; Tran, M. Q.; Harding, S. E.; Ali, N. N.; Boccaccini, A. R. *Biomaterials* **2008**, 29 (1), 47–57.

(6) (a) Grego, A. V.; Mingrone, G. *Clin Nutr* **1995**, *14* (3), 143-8; (b) Liu, G.; Hinch, B.; Beavis, A. D. *J. Biol. Chem.* **1996**, *271* (41), 25338–44.

(7) Sundback, C. A.; Shyu, J. Y.; Wang, Y.; Faquin, W. C.; Langer, R. S.; Vacanti, J. P.; Hadlock, T. A. *Biomaterials* **2005**, *26* (27), 5454–64.

(8) Langer, R.; Vacanti, J. P. *Science* **1993**, *260* (5110), 920–6.

(9) Freed, L. E.; Engelmayr, G. C., Jr.; Borenstein, J. T.; Moutos, F. T.; Guilak, F. *Adv. Mater.* **2009**, *21* (32-33), 3410–8.

(10) Ghosh, K.; Ingber, D. E. *Adv. Drug Deliv. Rev.* **2007**, *59* (13), 1306–18.

(11) (a) Crapo, P. M.; Gao, J.; Wang, Y. *J. Biomed. Mater. Res. A* **2008**, *86* (2), 354–63; (b) Crapo, P. M.; Wang, Y. *Biomaterials* **2010**, *31* (7), 1626–35; (c) Gao, J.; Crapo, P.; Nerem, R.; Wang, Y. *J. Biomed. Mater. Res. A* **2008**, *85* (4), 1120–8; (d) Gao, J.; Ensley, A. E.; Nerem, R. M.; Wang, Y. *J. Biomed. Mater. Res. A* **2007**, *83* (4), 1070–5.

(12) Wu, W.; Allen, R. A.; Wang, Y. *Nat. Med.* **2012**, *18* (7), 1148–53.

(13) Allen, R. A.; Wu, W.; Yao, M.; Dutta, D.; Duan, X.; Bachman, T. N.; Champion, H. C.; Stolz, D. B.; Robertson, A. M.; Kim, K.; Isenberg, J. S.; Wang, Y. *Biomaterials* **2014**, *35* (1), 165–73.

(14) (a) Engelmayr, G. C., Jr.; Cheng, M.; Bettinger, C. J.; Borenstein, J. T.; Langer, R.; Freed, L. E. *Nat. Mater.* **2008**, *7* (12), 1003–10; (b) Radisic, M.; Marsano, A.; Maidhof, R.; Wang, Y.; Vunjak-Novakovic, G. *Nat. Protoc.* **2008**, *3* (4), 719–38; (c) Radisic, M.; Park, H.; Chen, F.; Salazar-Lazzaro, J. E.; Wang, Y.; Dennis, R.; Langer, R.; Freed, L. E.; Vunjak-Novakovic, G. *Tissue Eng.* **2006**, *12* (8), 2077–91; (d) Radisic, M.; Park, H.; Martens, T. P.; Salazar-Lazaro, J. E.; Geng, W.; Wang, Y.; Langer, R.; Freed, L. E.; Vunjak-Novakovic, G. *J. Biomed. Mater. Res. A* **2008**, *86* (3), 713–24.

(15) Sales, V. L.; Engelmayr, G. C., Jr.; Johnson, J. A., Jr.; Gao, J.; Wang, Y.; Sacks, M. S.; Mayer, J. E., Jr. *Circulation* **2007**, *116* (11 Suppl), I55–63.

(16) Neeley, W. L.; Redenti, S.; Klassen, H.; Tao, S.; Desai, T.; Young, M. J.; Langer, R. *Biomaterials* **2008**, *29* (4), 418–26.

(17) Redenti, S.; Neeley, W. L.; Rompani, S.; Saigal, S.; Yang, J.; Klassen, H.; Langer, R.; Young, M. J. *Biomaterials* **2009**, *30* (20), 3405–14.

(18) Zaky, S. H.; Lee, K. W.; Gao, J.; Jensen, A.; Close, J.; Wang, Y.; Almarza, A. J.; Sfeir, C. *Tissue Eng. Part A* **2014**, *20* (1-2), 45–53.

(19) Engelmayr, G. C.; Cheng, M. Y.; Bettinger, C. J.; Borenstein, J. T.; Langer, R.; Freed, L. E. *Nat. Mater.* **2008**, *7* (12), 1003–1010.

For questions, product data, or new product suggestions, contact us at **matsci@sial.com**.

83

Poly(glycerol Sebacate)s

For more information on this product line, visit aldrich.com/biodegradable.

Name	Prod. No.
Regenerez Poly(glycerol sebacate) Resin	900210-25G

PLGA Biodegradable Polymers

For more information on these products, visit aldrich.com/biodegradable.

Low PDI Polylactides

Name	Structure	Molecular Weight (Avg M_n)	PDI	Degradation Time	Prod. No.
Poly(L-lactide)		10,000	≤1.1	>3 years	765112-5G
		5,000	≤1.2	>3 years	764590-5G
		20,000	≤1.1	>3 years	764698-5G
Poly(D,L-lactide)		5,000	≤1.1	<6 months	764612-5G
		10,000	≤1.2	<6 months	764620-5G
		20,000	≤1.3	<6 months	767344-5G

End-functionalized Low PDI Poly(L-lactide)s

Name	Structure	Molecular Weight (Avg M_n)	PDI	Prod. No.
Poly(L-lactide), acrylate terminated		5,500	≤1.2	775983-1G
		2,500	≤1.2	775991-1G
Poly(L-lactide), amine terminated		2,500	≤1.3	776378-1G 776378-5G
		4,000	≤1.2	776386-1G 776386-5G
Poly(L-lactide), azide terminated		5,000	<1.2	774146-1G
Poly(L-lactide) N-2-hydroxyethylmaleimide terminated		5,000	<1.2	746517-1G 746517-5G
		2,000	≤1.2	746797-1G 746797-5G
Poly(L-lactide) 2-hydroxyethyl, methacrylate terminated		5,500	≤1.2	766577-1G 766577-5G
		2,000	≤1.1	771473-1G 771473-5G
Poly(L-lactide), propargyl terminated		2,000	≤1.1	774162-1G
		5,000	≤1.1	774154-1G
Poly(L-lactide), thiol terminated		5,000	≤1.2	747394-1G 747394-5G
		2,500	≤1.2	747386-1G 747386-5G

Poly(lactide-*co*-glycolide) Copolymers

Name	Feed Ratio	End Group	Molecular Weight (Avg M_n)	Degradation Time (months)	Prod. No.
Poly(D,L-lactide-*co*-glycolide)-COOH	lactide:glycolide 85:15	-	17,000	-	798487-1G
Poly(D,L-lactide-*co*-glycolide)		ester terminated	50,000–75,000	<6	430471-1G 430471-5G
Resomer® RG 502, Poly(D,L-lactide-*co*-Glycolide)	lactide:glycolide 50:50	ester terminated	7,000–17,000	<3	719889-1G 719889-5G
Resomer® RG 502 H, Poly(D,L-lactide-*co*-glycolide)		acid terminated	7,000–17,000	<3	719897-1G 719897-5G
Resomer® RG 503, Poly(D,L-lactide-*co*-glycolide)		ester terminated	24,000–38,000	<3	739952-1G 739952-5G
Resomer® RG 503 H, Poly(D,L-lactide-*co*-glycolide)		acid terminated	24,000–38,000	<3	719870-1G 719870-5G
Resomer® RG 504, Poly(D,L-lactide-*co*-glycolide)		ester terminated	38,000–54,000	<3	739944-1G 739944-5G
Resomer® RG 504 H, Poly(D,L-lactide-*co*-gylcolide)		acid terminated	38,000–54,000	<3	719900-1G 719900-5G
Resomer® RG 505, Poly(D,L-lactide-*co*-glycolide)		ester terminated	54,000–69,000	<3	739960-1G 739960-5G
Resomer® RG 653 H, Poly(D,L-lactide-*co*-glycolide)	lactide:glycolide 65:35	acid terminated	24,000–38,000	<5	719862-1G 719862-5G
Resomer® RG 752 H, Poly(D,L-lactide-*co*-glycolide)	lactide:glycolide 75:25	acid terminated	4,000–15,000	<6	719919-1G 719919-5G
Resomer® RG 756 S, Poly(D,L-lactide-*co*-glycolide)		ester terminated	76,000–115,000	<6	719927-1G 719927-5G
Resomer® RG 858 S, Poly(D,L-lactide-*co*-glycolide)	lactide:glycolide 85:15	ester terminated	190,000–240,000	<9	739979-1G 739979-5G

CHITOSAN BIOPOLYMER FROM FUNGAL FERMENTATION
FOR DELIVERY OF CHEMOTHERAPEUTIC AGENTS

David Brown,[1] Keith Brunt,[2] Nils Rehmann[3]
[1]CTO Mycodev Group, Fredericton, NB E3B 6B3 Canada
[2]Dalhousie School of Medicine New Brunswick, Saint John, NB E2K 5E2, Canada
[3]NiRem Consulting, 8 Fish Hatchery Lane, French Village, NB E3E 2H5, Canada
Email: Dave@mycodevgroup.com,[1] Nils@nirem.ca[3]

Introduction

Chitosan is a naturally occurring polysaccharide ideally suited for use in medical supplies, devices, therapeutics, and diagnostics. The unique natural characteristics of chitosan include its cationic, biocompatible, biodegradable, non-toxic, non-immunogenic, and antimicrobial properties. Chitosan is predominantly extracted from shellfish waste in developing countries with limited oversight. This causes inconsistencies in molecular weight and purity and allows the introduction of contaminates such as heavy metals in crustacean-derived chitosan. Shellfish allergen protein, such as tropomysin, and high levels of heavy metals, such as mercury and arsenic, may be present in crustacean chitosans, particularly those sourced from regions with high levels of pollution. This lack of product control results in significant risk of reticent anaphylaxis thus, limiting its clinical use. Another production-related issue in the use of chitosan produced from shellfish is the seasonality of the industrial harvest. An alternative approach is the fermentation of fungal chitosan. Pharmaceutical-grade chitosan can be produced from fungi using a submerged fermentation process in a highly controlled and standardized production method using good manufacturing processes (GMP), to produce material acceptable for medical use in drug delivery and other life science applications. Chitosan is a cationic polysaccharide composed of β(1-4) linked glucosamine and *N*-acetyl glucosamine units[1] (**Figure 1**). Fermentation is a preferred method for production of many clinical compounds due to the ease in which biochemically controlled and standardized engineering conditions can be met, offering an optimal method for the production of chitosan for medical applications.
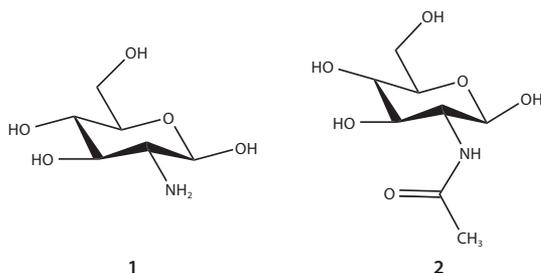
Fungal Fermentation for Chitosan Production

Chitin is second only to cellulose as the most abundant biopolymer found in nature. Chitin and its derivative chitosan are naturally produced in fungi as the principal component of the cell walls.[2] Chitin and chitosan production in the cell wall is a complex biosynthetic process performed by different families of chitin synthase (CHS) enzymes. A portion of the synthesized chitin is deacetylated to chitosan by the enzyme chitin deacetylase.[3] The submerged fermentation of the fungus allows for tightly controlled production of chitosan and limits exposure to foreign material and other organisms.

Mycodev Group, a company producing pharmaceutical-grade fungal-derived chitosan, uses a proprietary species of filamentous fungus to produce chitosan using submerged fermentation. While the use of this approach is the first in the chitosan industry, it has been envisioned for some time.

For example, George Roberts of the University of Nottingham mentioned the process in a 2008 review on fungal production stating that this fermentation would offer a stable, non-seasonal source of raw material that is more consistent in character than shellfish waste.[4] The aforementioned concerns with shellfish allergen protein and high levels of heavy metals are not applicable to fungal chitosan

Production of Specific Molecular Weights and Percent Degree of Deacetylation

The most important characteristics in determining the functionality of chitosan are degree of deacetylation (%DDA) and molecular weight (M_w). Chitosan is technically defined as chitin with more than 60% DDA.[6] Chitosan with higher %DDA possesses more positively charged amine groups when dissolved in solution.[7] In traditionally sourced crustacean based chitosan production, large volumes of high temperature, caustic solution are required to chemically remove the acetyl groups. Fungal production of chitosan allows for very high %DDA values due to the nature of the fermentation, with the ability to routinely produce a DDA as high as 99%.

The average M_w of chitosan is also a very important characteristic. Similar to most polymers, the M_w of chitosan impacts the viscosity of the chitosan solution, whereby increases in the M_w of chitosan raises the viscosity of the solution. Chitosan properties such as biodegradability, mucoadhesion,

Figure 1. The glucosamine (**1**) and *N*-acetyl glucosamine (**2**) units of chitosan biopolymer.

hemostatic, antimicrobial, anticholesterolemic, and antioxidant ability are all highly dependent on M_w.[8] Many applications require covalent or ionic crosslinking of chitosan to other molecules, with the M_w cited as a critical factor in successful chemical conjugation.[9] The M_w consistency of chitosan has long been a hurdle to commercial reproducibility and repeatability, significantly hindering the translation of academic studies into commercial applications. Sophisticated applications where chitosan interacts with other substances also suffer from inconsistent results when chitosan with high levels of batch-to-batch M_w variability are used. While crustacean-based production of chitosan exhibits a high degree of batch-to-batch variance in M_w (and difficulty in separating different molecular weights),[10] fermentation provides conditions for fungal biomass production with a predictable chitosan M_w. For example, the polydispersity index (PDI) is known to be much lower in fungal-sourced chitosan, improving the performance and reproducibility of many chitosan applications. **Figure 2** shows a representation of the M_w distribution of fungal chitosan vs. large PDI chitosan from traditional crustacean source methods.
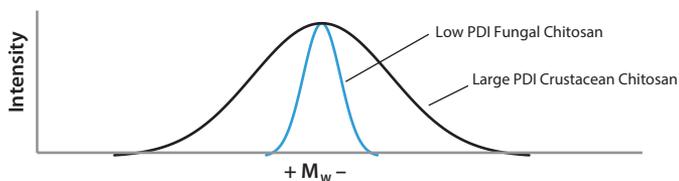

Figure 2. A representation of the polydispersity index (PDI) of chitosan from fungal and crustacean sources. Fungal chitosan typically has a low PDI compared to crustacean-sourced chitosan.

The variability of fermentation, such as time, temperature, pH, nutrients, aeration, and mixing, all affect the M_w and PDI of chitosan, yet strict control of these parameters ensures a high degree of reproducibility of the chitosan M_w and %DDA. Consistent M_w and %DDA is critical for the use and acceptance of chitosan in medical and pharmaceutical applications and allows for less variability in research, development, and subsequent commercialization. Fungal chitosan production by fermentation also allows for control of the M_w, allowing the ability to produce a specific M_w to fulfil specific application requirements. Technology developed by Mycodev Group has allowed production of different molecular weights directly as a result of the controlled fermentation process (reproducibly from batch to batch). Through fermentation, molecular weights from as low as 5 kDa to as high as 500 kDa, and any molecular weight in between, can be routinely produced. This ability has become essential for enabling the development of specific chitosan applications and securing paths to commercialization that previously seemed unreachable using the traditional chitosan supply.

Chitosan for Delivery of Chemotherapeutic Agents

Chemotherapy and targeted therapy combinations have helped to significantly improve patient outcomes in the last decade. Though chemotherapeutic agents can be highly effective, systemic administration of these agents has significant adverse side effects on healthy cells, and causes negative physical effects including nausea, hair loss, compromised immune system, cardiotoxicity, and nervous system damage.[11]

Contained delivery of chemotherapy to cancer-site specific areas reduces or eliminates many detrimental side effects. Additionally, higher concentrations of agents adequately titrated for delivery to a highly specific target area reduce the risk of chemoresistance.[12] Polymer and biopolymer drug delivery systems in the form of nanoparticles, films, gels, wafers, and rods have been investigated for their ability to localize chemotherapy administration.[13] Biopolymers like chitosan that are biodegradable and can be metabolized from the body are clinically attractive for use in drug delivery. The biocompatibility of chitosan is dependent on the sterility, purity, molecular weight, and percent degree of deacetylation.[14]

Paclitaxel Encapsulation with ZnO and Modified Chitosan

A recent study using chitosan in combination with ZnO nanocarriers containing the chemotherapy agent paclitaxel (PAC) to target breast cancer tumors gives further insight into the use of chitosan nanoparticles in drug delivery methods. Paclitaxel, a member of the taxane drug class, is limited in the dose that can be provided due to its poor solubility[15] and toxicity towards healthy tissues. It was hypothesized that a controlled and localized release of paclitaxel would improve its overall therapeutic efficacy. ZnO as a nanocarrier had still limitations including agglomeration,[16] metal oxide toxicity,[17] and immune reactivity; however, when chitosan was used as a surface-tethering agent researchers were able to overcome these limitations.

Chitosan-ZnO nanocarriers were conjugated using click chemistry with the alkyne derivative of folic acid for targeted uptake by overexpressed folate receptors in breast cancer tumors (**Figure 3**). As the chitosan-ZnO nanocarriers arrive in the tumor microenvironment, their surface charge becomes positive, promoting uptake either through surface binding or through folate receptor internalization into the endolysome. Upon delivery, the highly acidic milieu causes the nanocarriers to collapse
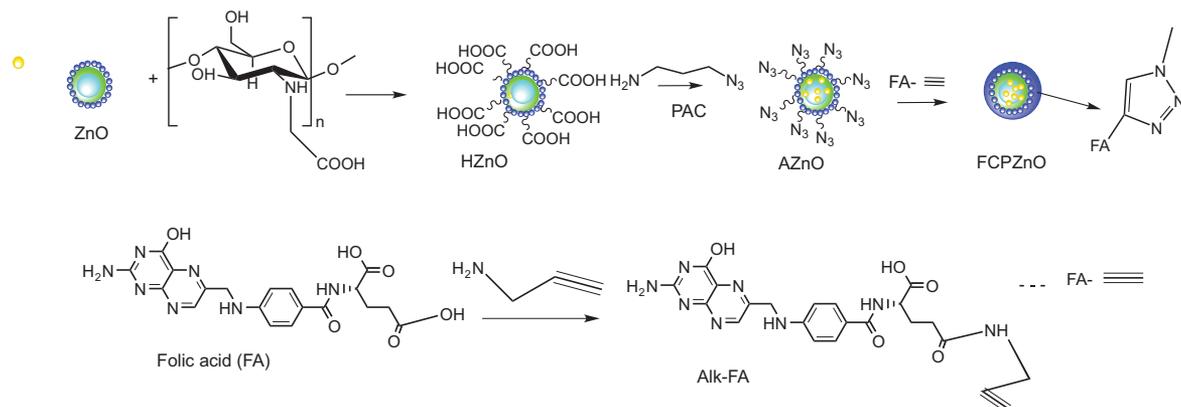

Figure 3. Schematic representation of the approach used to functionalize folic acid through the click chemistry approach for the paclitaxel encapsulated ZnO spheres. Reprinted with permission from *Nature Scientific Reports* 2015, *5*.

and release their payload of paclitaxel. As a unique consequence of this collapse, the nanoparticle fluoresces differentially, enabling potential future use in imaging tumor drug titration.

In order to test the effectiveness of the chitosan-ZnO nanocarriers, 6–7 week old female athymic BALB/c (nu+/nu+) mice were injected subcutaneously with human MDA-MB-231 adenocarcinoma cells. The paclitaxel-loaded nanocarriers (termed FCPZnO) were tested alongside native paclitaxel, and hollow chitosan-ZnO nanocarriers (HZnO). Tagging IRDye 680 to the FCPZnO prior to the intravenous delivery to the tail vein allowed the researchers to use *in vivo* fluorescence imaging to track particle uptake to the tumor (**Figure 4**).

Use of fluorescence imaging made clear that the targeting of the FCPZnO particles to the site of the tumor was significant. The investigators concluded that the preference for folate surface functionalization of the breast cancer cells and the charge repulsion between the healthy tissue and the nanocarriers allowed for the successful delivery of the paclitaxel chemotherapy. Within hours of delivery, FCPZnO was accumulating within the tumor and had a greater than 3-fold efficacy in eliminating tumor volume and mass compared to the control.

Conclusion

Improving the bioavailability of drugs through novel nanocarrier drug delivery systems is possible through the use of biocompatible substrates like high purity, fungal-derived chitosan. Achieving localized delivery reduces the negative side effects of paclitaxel and proves to be highly effective at eliminating the volume and mass of breast cancer cells in mice. A wide range of drug delivery applications can be enhanced by chitosan prepared either as a hydrogel or as nanoparticles, where the polycationic amino groups interact with the drug's anionic groups. Chitosan produced by fermentation provides these applications with improved purity and consistency, as well as the opportunity to use specific M_w and %DDA to further optimize the performance and reproducibility.

References

(1) Pillai, C.; Paul, W.; Sharma, C. *Prog. Polym. Sci.* **2009**, *34*, 641–678.
(2) Lenardon, M.; Munro, C.; Gow, N. *Curr Opin Microbiol.* **2010**, *13*(4), 416–423.
(3) Jeraj, N.; Kunic, B.; Lenasi, H.; Breskvar, K. *Enzyme Microb. Technol.* **2006**, *6*(3), 1294–1299.
(4) Roberts, G. *Progress in the Chemistry and Application of Chitin and its Derivatives.* **2008**, *11*, 7–15.
(5) Riva, R.; Ragelle, H.; des Rieux, A.; Duhem, N.; Jerome, C.; Preat, V. *Adv. Polym. Sci.* **2011**, 19–44.
(6) Rinaudo, M. *Prog. Polym. Sci.* **2006**, 603–632.
(7) Alsarra, L.; Betigeri, S.; Zhang, H.; Evans, B.; Neau, S. *Biomaterials* **2002**, *23*(17), 3637–3644.
(8) Aranaz, I.; Mengibar, M.; Harris, R.; Panos, I.; Miralles, B.; Acosta, N.; Galed, G.; Heras, A. *Curr. Chem. Biol* **2009**, *3*(2), 203–230.
(9) Honary, S.; Hoseinzadeh, B.; Shalchian, P. *Trop. J. Pharm. Res.* **2010**, *9*(6), 525–531.
(10) Hamilton, V.; Yuan, Y.; Rigney, D.; Puckett, A.; Ong, J.; Yang, Y.; Elder, S.; Bumgardner, J. *J. Mater. Sci. Mater. Med.* **2006**, *17*(12), 1373–1381.
(11) Meyers, C. *Journal of Biology* **2008**, *7*(11).
(12) Basile, K.; Aplin, A. *Adv. Pharmacol.* **2012**, *65*, 315–334.
(13) Wolinsky, J.; Colson, Y.; Grinstaff, M. *J. Control. Release.* **2012**, *159*(1), 1000–1016.
(14) Rodrigues, S.; Dionisio, M.; Lopez, C.; Crenha, A. *J. Funct. Biomater.* **2012**, *3*, 615–641.
(15) Ghaz-Jahanian, M.; Abbaspour-Aghdam, F.; Anarjan, N.; Berenjian, A.; Jafarizadeh-Malmiri, H. *Mol. Biotechnol.* **2015**, *57*(3), 201–218.
(16) Huang, C.; Aronstam, R.; Chen, D.; Huang, Y. *Toxicol. In Vitro*, **2010**, *24*(1), 45–55.
(17) Jeng, H.; Swanson, J. *J. Environ. Sci. Health., Part A.* **2006**, *41*(12), 2699–2711.
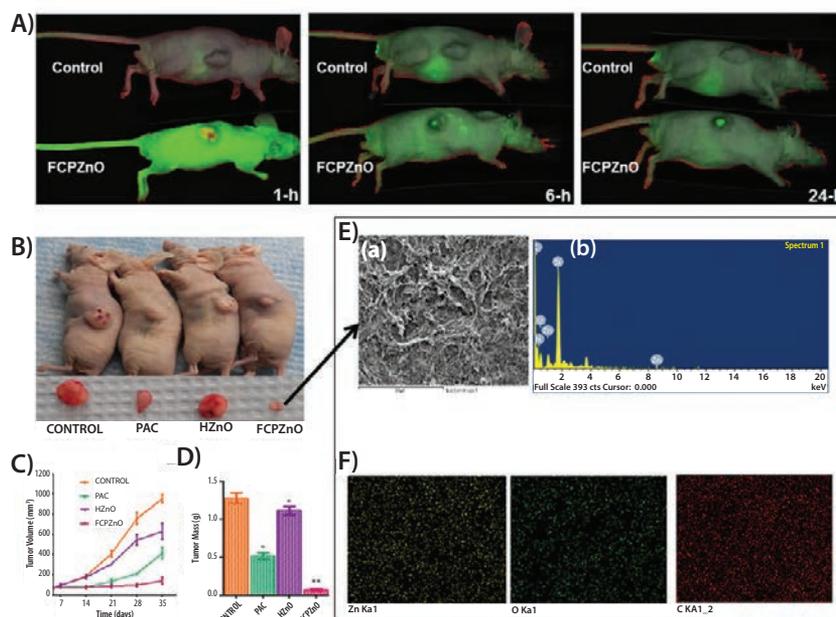
Figure 4. Regression of MDA-MB-231 tumor xenografts in mice treated with FCPZnO and PAC. **A)** *In vivo* real-time images of IRDye 680-labeled FCPZnO compared to control (IRDye 680). **B)** Drug treatment groups received PAC (10 mg/kg, intravenous or iv), equivalent dose of PAC in nanoformulation (10 mg/kg, iv), and equivalent weight of nanocarrier (iv). Tumor volumes in the FCPZnO group were significantly diminished in comparison with free PAC at 35 days after treatment (P <0.05). **C)** Tumor volume, **D)** Tumor mass, and **E)** Spectral shift of tumor sections of FCPZnO-treated mice (**A** and **B**). **F)** FESEM image of tumor cross section area for EDX elemental mapping of corresponding sample zinc (yellow), oxygen (green) and carbon (red) and corresponding EDX spectra. Reprinted with permission from *Nature Scientific Reports* **2015**, *5*.

Non-animal Derived Chitosans

For a complete list of available materials, visit aldrich.com/natural.

Name	Molecular Weight (Avg M_w)	Degree Of Deacetylation	Prod. No.
Chitosan	5,000 Da	≥80% deacetylated	900345-2G
	50 kDa	≥80% deacetylated	900341-2G
	100 kDa	99% deacetylated	900344-2G
	100 kDa	≥80% deacetylated	900342-2G
	180 kDa	≥80% deacetylated	900343-2G

Natural Polymers

For a complete list of available materials, visit aldrich.com/natural.

Name	Inherent Viscosity (cP)	Degree Of Deacetylation	Prod. No.
Alginic acid	15–25 1 % in H_2O	-	180947-100G 180947-250G 180947-500G
Chitosan	20–300 (1 wt. % in 1% acetic acid Brookfield)	75–85% deacetylated	448869-50G 448869-250G
	200–800 (1 wt. % in 1% acetic acid Brookfield)	75–85% deacetylated	448877-50G 448877-250G
	800–2,000 (1 wt. % in 1% acetic acid Brookfield)	>75% deacetylated	419419-50G 419419-250G

HIGH-PURITY COLLAGEN

Collagen is biocompatible, biodegradable, and contains biological recognition sequences that promote cell migration, attachment, and proliferation. These can be exploited for tissue regeneration and site-specific drug delivery. We offer a selection of high purity, biocompatible, and biodegradable collagen to enable biomedical research.

Features
- Type I, Bovine Corium
- Pepsin (atelo) and acid (telo) solubilized available
- High purity
- Low endotoxin

Applications
- 3D scaffolds
- Regenerative medicine
- Medical devices and implants
- Drug delivery
- *In vitro* diagnostics

High-purity Collagen Products[*]

Name	Prod. No.
Type I Bovine Collagen Solution, Pepsin soluble, 3 mg/mL, ≥95% purity	804592
Type I Bovine Collagen Solution, Pepsin soluble, 6 mg/mL, ≥95% purity	804622
Type I Bovine Collagen Solution, Acid Soluble telocollagen, 6 mg/mL, ≥95% purity	804614

*Products of Collagen Solutions Plc

Learn more about natural polymers and applications, including our complete product offering, at
aldrich.com/natural

APPLICATIONS OF Y-SHAPE PEG DERIVATIVES FOR DRUG DELIVERY

Dr. Hui Zhu
JenKem Technology Co. Ltd., Beijing, P.R. China
Email: tech@jenkemusa.com

Introduction

The immune system protects the body from disease by resisting the invasion of foreign molecules into its cells, for example peptides and proteins are hydrolyzed by proteolytic enzymes; nucleic acids are hydrolyzed by nucleases; and most small molecules are eliminated in the liver and kidneys. This immune reaction protects the body from disease but can also cause many drugs to become inactive. PEGylation is one of the most common methods of drug delivery employed to prolong elimination half-life and reduce drug immunogenicity.

Polyethylene glycol (PEG) is a water-soluble synthetic polymer consisting of repeating ethoxy units: $-(CH_2-CH_2-O)-$. PEGylation, the covalent conjugation of a PEG derivative to another molecule, has proven to be a safe and effective method of drug modification for drug delivery applications and has gained acceptance by regulatory agencies for use in a variety of commercialized products. PEGylation can protect a drug from being hydrolyzed by enzymes, improve the Pharmacokinetic/Pharmacodynamic (PK/PD) profile and stability, and reduce drug toxicity while increasing water solubility.

Based on molecular structure, PEG materials can be classified into three main categories: linear PEGs, multi-arm PEGs, and branched PEGs (**Figure 1**). Linear PEGs such as methoxy PEGs (mPEGs), as well as hetero- and homo-bifunctional PEGs, are used frequently for PEGylation of peptides, proteins, siRNA and modification of other small molecules, and for preparation of drug delivery systems such as nanoparticles. Multi-arm PEGs have similar physicochemical properties as linear PEGs, are used to increase drug loading and are used in the preparation of hydrogels by crosslinking.[1] PEGylation with branched mPEG chains provides improved stability against enzymatic digestion compared to PEGylation with linear PEGs.[2–4]

There are two types of branched PEG materials currently used in the market: U-shape PEGs and Y-shape PEGs (**Figure 2**). The stability of the enzymes ribonuclease, catalase, asparaginase, and trypsin to proteases after modification with U-shape PEGs and linear PEGs was compared by Monfardini et al.[2] at different pH and temperatures. Their results showed that U-shape PEG-modified enzymes exhibited better stability than linear PEGs. Zhou et al.[3,4] reported that *in vitro* pharmaceutical activity of the

Y-shape PEG modified proteins, interferon α2a, α2b and rhGH, is higher than that of U-shape PEG modified enzymes, potentially as a result of the difference in the chemical structure of the two branched PEGs (**Figure 2**).
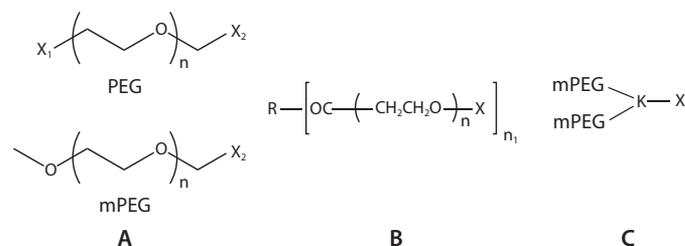
Legend

X, X_1, X_2:	Functional groups, i.e., NHS, NH$_2$, COOH, or Maleimide
R:	The core molecule for multi-arm PEGs, such as tripentaerythritol for 8arm PEGs
n:	Number of repeating (CH$_2$CH$_2$O) units
n$_1$:	Number of PEG arms, usually 3, 4, 6 or 8
K:	Linker for branched PEGs

Figure 1. Common structures of PEGs: **A**) linear PEGs; **B**) multi-arm PEGs; and **C**) branched PEGs.
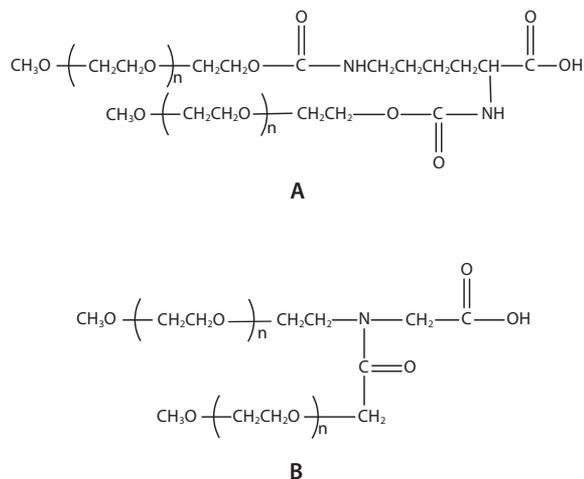
Figure 2. Example structures of branched PEGs: **A**) U-shape PEG and **B**) JenKem Technology's patented Y-shape PEG.

For these reasons, the application of branched mPEG derivatives in the biomedical field is attracting more attention. This review is focused on several applications of Y-shape PEG derivatives in the biopharmaceutical area, including applications for PEGylation of cancer therapeutics, cocaine esterase, antibiotics, and antivirals. **Table 1** summarizes the applications of Y-shape PEG derivatives for drug delivery.

Table 1. Applications of Y-shape PEGs for drug modification.

Drug Modified with Y-shape PEG	Y-shape PEG Employed for Drug Delivery	Refs.
Cocaine esterase	Maleimide; M_W 40,000 Da	14,15
Cp40	NHS; M_W 40,000 Da	18
DNA aptamer (SOMAmer)	NHS; M_W 40,000 Da	16
G-CSF	NHS; M_W 40,000 Da	10
Gentamicin	NHS; M_W 40,000 Da	12
IFN-α2a	NHS; M_W 40,000 Da	3
IFN-α2b	NHS; M_W 40,000 Da	4
Laccase	Propionaldehyde; M_W 40,000 Da	9
LIF receptor antagonist (LA)	NHS; M_W 40,000 Da	20
L-RNA (Spiegelmer)	NHS; M_W 40,000 Da	11
L-RNA (Spiegelmer)	NHS; M_W 40,000 Da	17
rhGH	NHS; M_W 40,000 Da	19
Paclitaxel	Amine; M_W 40,000 Da	6
siRNA	Maleimide; M_W 20,000 Da	5
TNF-α	NHS; M_W 40,000 Da	7,8

Applications of Y-shape PEGs for PEGylation of Cancer Therapeutics

Many molecules with antitumor activity require modification prior to their use in cancer treatment due to their hydrophobicity, short half-life, toxicity, and immunogenicity. PEGylation enables the use of these molecules in the treatment of cancer by reducing or avoiding these negative attributes. Several PEG-modified drugs (such as Caelyx™, PegIntron®, CIMZIA®, PEGASYS®, and Oncaspar™) are already on the market, while many others are in different stages of clinical research studies.

Progress on research and development of a number of cancer therapeutics modified using Y-shape PEGs has recently been reported. For example, Li et al.[5] developed dual MMP7 (matrix metalloproteinase 7) proximity-activated and folate receptor-targeted nanoparticles (NPs) for siRNA delivery. This siRNA nanocarrier, which forms a pH-responsive, endosomolytic core and two coronas, is self-assembled from two polymers, folic acid (FA)-PEG and Y-shape PEG-PAT (proximity-activated targeting, MMP-cleavable peptide). The corona of the Y-shape PEG shields against nonspecific interactions within the blood. When PAT is cleaved within an MMP-rich environment (such as inside metastatic cancer tissues), the Y-shape PEG is removed, exposing the underlying FA and making it accessible for folate receptor-mediated NP uptake. Using breast cancer cells as a target, the authors noted that the NPs show undetectable levels of cytotoxicity, whereas the protein-level knockdown of a model gene is greater than 50%.

In a different example using Y-shape PEG modified nanoparticles, Amoozgar et al.[6] used Y-shape PEG Amine as a surface coating on paclitaxel-loaded nanoparticles. They found that the NPs significantly extended the survival time of ovarian tumor-bearing mice treated with NPs by 1–2 weeks.

Y-shape PEG-TNF-α and Y-shape PEG-vcTNF-α, both of which use a cathepsin B-sensitive dipeptide (valine-citrulline, vc) to link Y-shape PEG and TNF-α, were prepared by Dai et al.[7,8] Tumor necrosis factor-α (TNF-α) has a very potent biological activity and is used to directly kill tumor cells. However, its medical application is limited due to serious side effects, rapid clearance from circulation, and unspecific distribution among tissues after intravenous administration. Researchers found

that Y-shape PEG-vcTNF-α induces higher cytotoxicity and an ~10-fold increase in antitumor activity compared to Y-shape PEG-TNF-α. *In vivo* pharmacokinetics studies demonstrated that the half-life of Y-shape PEG-vcTNF-α is similar to Y-shape PEG-TNF-α and 70-fold longer than that of native TNF-α.[7] Another cathepsin B-sensitive Y-shape PEG-modified TNF-α (Y-shape PEG-vc-PABC- TNF-α, Y-shape PEG-vc containing a *p*-amino benzyl carbonyl spacer) showed similar properties.[8]

Deloisa et al.[9] studied the PEGylation reaction of laccase and the enzymatic activity of PEG-laccase. Laccase is a copper-containing oxidoreductase that catalyzes the oxidation of phenolic compounds with antiproliferative activity toward tumor cells. The researchers found that neither molecular weight nor type of PEG structure (such as linear or branched) had a significant impact on the laccase activity. After PEGylation, the laccase activity with ABTS (2,2′-azino-bis(3-ethylbenzothiazoline-6-sulfonic acid)) was maintained at nearly 100%.

The protein G-CSF stimulates the survival, proliferation, differentiation, and function of hematopoietic cells. A recombinant form of G-CSF can be employed as an adjuvant to certain cancer therapies to accelerate recovery from neutropenia after chemotherapy, allowing higher-intensity treatment. Wang et al.[10] synthesized Y-shape PEG-modified G-CSF using lysine-specific PEGylation. In the mouse study of the treatment for *in vivo* 5-fluorouracil-induced neutropenia, Y-shape PEG-G-CSF showed less dosing frequency and dosage compared to Filgrastim™. The half-life of Y-shape PEG-G-CSF was 19-fold longer than Filgrastim™ as measured in cynomolgus monkeys.

Bone marrow (BM) metastasis is the main cause of death associated with multiple myeloma (MM). Roccaro et al.[11] reported that stromal cell derived factor 1, SDF-1, also known as CXCL12, a small molecule cytokine, is highly expressed in active MM and BM sites of tumor metastasis. The researchers produced a high-affinity anti-SDF-1 L-oligonucleotide PEGylated with Y-shape PEG (olaptesed-pegol, ola-PEG), using mirror-image phage display and Spiegelmers technology. The survival time of mice treated with ola-PEG was shown to be longer by about 2 weeks than that of untreated mice, with significant reduction of MM cell tumor growth. SDF-1 neutralization with ola-PEG in BM niches of mouse models leads to reduced MM cell homing and growth, thereby inhibiting MM disease progression.

Applications of Y-shape PEGs for PEGylation of Antibiotics and Antivirals

Y-shape PEGs have been employed for PEGylation of antibiotics and antivirals that exhibit *in vivo* stability problems. Marcus et al.[12] developed a reversible PEGylation process for gentamicin. Reversibly PEG-modified drugs are capable of prolonged drug release *in vivo* while retaining drug activity of the unmodified drug. For example, PEG-gentamicin regains full antibacterial potency upon incubation *in vitro*; following systemic administration to rats, the half-life of PEG-gentamicins are 7 to 15-fold greater than the half-life of systemically administered nonderivatized gentamicin.

Interferon (IFN) is a broad-spectrum antiviral agent that indirectly suppresses a virus by producing antiviral protein through cell surface receptors to inhibit viral replication. IFN can also enhance the activity of natural killer cells (NK cells), macrophages, and T lymphocytes and the effectiveness of antivirals. For example, Zhou et al.[3,4] describe the development of Y-shape PEG-IFN α2a and Y-shape PEG-IFN α2b. The *in vivo* half-lives of Y-shape PEG-IFNs were more than 10-fold longer than the half-life of the unmodified IFN, as measured in cynomolgus monkeys.

Additionally, Y-shape PEG-IFNs induced a 2 to 3-fold increase of antiviral activity *in vitro*, compared to PEGASYS® (PEG Interferon α-2a).

Applications of Y-shape PEGs for PEGylation of Cocaine Esterase

Cocaine esterase (CocE) is regarded as the most efficient native enzyme for cocaine degradation. Enhancing cocaine metabolism by administration of cocaine esterase is considered to be a promising treatment strategy for cocaine overdose and addiction. However, its thermo-instability, rapid degradation by circulating proteases, and potential immunogenicity limits the application of cocaine esterase in medicine.[13]

Narasimhan et al.[14] report that the T172R/G173Q mutant of cocaine esterase (CCRQ-CocE) improves its *in vivo* residence time from 24 to 72 h when it is modified by Y-shape PEG. CCRQ-CocE has an improved thermostability, retaining over 90% of its activity after 41 days at 37 °C, while the *in vitro* half-life of wild-type cocaine esterase was only 12 min at 37 °C.

Through molecular modeling and dynamics simulation, Fang et al.[15] designed and characterized a promising new mutant of E172–173 with extra L196C/I301C mutations, denoted as enzyme E196–301. *In vivo* tests showed that Y-shape PEGylated E196–301 could fully protect mice from a lethal dose of cocaine of 180 mg/kg, LD_{100}, for at least 3 days, whereas the unPEGylated E196–301 could only protect mice for less than 24 h.

Other Applications of Y-shape PEGs for PEGylation

Y-shape PEGs have also been employed for PEGylation of nucleotides, Cp40, and rhGH, with applications in the treatment of rheumatoid disease, transplant health, and tissue growth.

Interleukin 6, or IL-6, stimulates and involves cellular proliferation, differentiation, and function of immune response. IL-6 and IL-1 are involved in the inflammatory response and fever reaction. SL1026, modified by Y-shape PEG, is a slow off-rate modified aptamer, SOMAmer, antagonist of IL-6, which neutralizes IL-6 signaling *in vitro* and delays the onset and reduces the severity of rheumatoid symptoms, per Hirota et al.[16] Administration of SL1026 in cynomolgus monkeys delays the progression of arthritis. SL1026 also inhibits IL-6-induced STAT3 phosphorylation *ex vivo* in T lymphocytes from human blood and IL-6-induced C-reactive protein and serum amyloid A production in human primary hepatocytes. The reported therapeutic effects of SL1026 are similar or slightly better than tocilizumab, which makes it a potential agent for the treatment of rheumatoid arthritis.

Complement component 3 (C3) inhibition is known to be vasculo-protective in transplantation studies. In the genetic absence of C3, however, complement component 5 (C5) convertase activity leads to the generation of C5a (anaphylatoxin), a promoter of vasodilatation and permeability. Khan et al.[17] prepared a specific C5a inhibitor, NOX-D19, a 44 nucleotide L-RNA modified by Y-shape PEG, and found that therapy with this agent prevents microvascular pathology. Since microvascular

dilatation and permeability increases during allograft rejection, vascular integrity is an important indicator of transplant health.

Ristano et al.[18] investigated the effect of Cp40 and Y-shape PEG-Cp40 on hemolysis and opsonization of PNH erythrocytes *in vitro* and *in vivo*. Cp40 and Y-shape PEG-Cp40 show the same inhibitory potency of hemolysis (IC ~4 μM; full inhibition ~6 μM) on erythrocytes from 2 untreated PNH patients. The elimination half-life of Y-shape PEG-Cp40 in nonhuman primates was more than 5 days, which is 10-fold longer than that of unmodified Cp40, which may potentially affect the plasma levels of C3.

Human growth hormone rhGH, produced by recombinant DNA technology, promotes cell reproduction, regeneration, and tissue growth. Zhou et al.[19] synthesized Y-shape PEG-rhGH with a resulting biological activity 1.5-fold higher than native rhGH in hypophysectomized rats. Further, the half-life of Y-shape PEG-rhGH measured in cynomolgus monkeys was more than 20-fold longer than the biological activity and half-life of native rhGH.

Conclusions

As evidenced in this review, drugs modified with the use of Y-shape PEGs exhibit better stability to enzymatic digestion, temperature, and pH, compared to linear PEG-modified and native drugs. PEGylation with Y-shape PEGs improves the PK/PD profile of the drugs. Reversible Y-shape PEGylation of drugs and drug delivery systems increase the activity and targeting compared to irreversible Y-shape PEGylation in cases where PEGylation of drugs inhibits their activity by blocking the active sites.

References

(1) Hutanu, D.; Frishberg, M.; Guo, L.; Darie, C. *Mod. Chem. Appl.* **2014**, *2*, 132.
(2) Monfardini, C.; Schiavon, O.; Caliceti, P.; Morpurgo, M.; Harris, J. M.; Veronese, F. *Bioconjugate Chem.* **1995**, *6*, 62–69.
(3) Zhou, W. et al. Interferon alpha 2a modified by polyethylene glycol, its synthesis process and application. Patent CN200780050541. **2007**.
(4) Zhou, W. et al. Interferon alpha 2b modified by polyethylene glycol, its synthesis process and application. Patent CN200780050542. **2007**.
(5) Li, H.; Miteva, M.; Kirkbride, K. C.; Cheng, M. J.; Nelson, C. E.; Simpson, E. M.; Gupta, M. K.; Duvall, C. L.; Giorgio, T. D. *Biomacromolecules*. **2015**, *16*, 192–201.
(6) Amoozgar, Z.; Wang, L.; Brandstoetter, T.; Wallis, S. S.; Wilson, E. M.; Goldberg, M. S. *Biomacromolecules*. **2014**, *15*, 4187–4194.
(7) Dai, C.-Y.; Fu, Y.; Li, B.; Wang, Y.-G.; Zhang, X.; Wang, J.-C.; Zhang, Q. *Sci. China Life Sci.* **2011**, *55*, 128–138.
(8) Dai, C.; Fu, Y.; Chen, S.; Li, B.; Yao, B.; Liu, W.; Zhu, L.; Chen, N.; Chen, J.; Zhang, Q. *Sci. China Life Sci.* **2013**, *56* (1), 51.
(9) Mayolo-Deloisa, K.; González-González, M.; Simental-Martínez, J.; Rito-Palomares, M. *J. Mol. Recognit.* **2015**, *28*: 173.
(10) Shiyuan Wang, S. et al. Y-type polyethylene glycol modified G-CSF and preparation method and use thereof. Patent CN200780051378. **2007**.
(11) Roccaro, A. M.; Sacco, A.; Purschke, W. G.; Moschetta, M.; Buchner, K. *Cell Reports* **2014**, *9*, 118.
(12) Marcus, Y.; Sasson, K.; Shechter, Y. *J. Med. Chem.* **2008**, *51*, 4300.
(13) Park, J. B.; Kwon, Y. M.; Lee, T. Y.; Ko, M. C.; Sunahara, R. K.; Woods, J. H.; Yang, V.C. *J. Control Release* **2010**, *142*, 174.
(14) Narasimhan, D.; Collins, G. T.; Nance, M. R.; Nichols, J.; Edwald, E.; Chan, J.; Ko, M. C.; Woods, J. H.; Tesmer, J. J.; Sunahara, R. K. *Mol. Pharmacol.* **2011**, *80*, 1056.
(15) Fang, L.; Chow, K. M.; Hou, S.; Xue, L.; Chen, X.; Rodgers, D. W.; Zheng, F.; Zhan, C. G. *ACS Chem. Biol.* **2014**, *9*, 1764.
(16) Hirota, M.; Murakami, I.; Ishikawa, Y.; Suzuki, T.; Sumida, S. et al. *Nucleic Acid Therapeutics* **2016**, *26*, 10.
(17) Khana, M.; Maasch, C.; Vater, A.; Klussmann, S.; Morser, J.; Leung, L. L.; Atkinson, C.; Tomlinson, S.; Heeger, P. S.; Nicolls, M. R. *PNAS* **2013**, *110*, 6061.
(18) Risitano, A. M.; Ricklin, D.; Huang, Y.; Reis, E. S.; Chen, H. et al. *Blood* **2014**, *123*, 2094.
(19) Zhou, W. et al. Double-stranded polyethylene glycol modified growth hormone, preparation method and application thereof. Patent CN200880009718. **2008**.
(20) Menkhorst, E.; Zhang, J.-G.; Sims, N. A.; Morgan, P. O. et al. *PLoS ONE* **2011**, *6*, e19665.

Poly(ethylene Glycol)s (PEGs)

For a complete list of available materials, visit aldrich.com/peg.

4arm PEGs

Name	Prod. No.
Average M_n 2,000	
4arm-PEG2K-NH2	JKA7032-1G
Average M_n 5,000	
4arm-PEG5K-COOH	JKA7109-1G
4arm-PEG5K-NH2 HCl Salt	JKA7020-1G
4arm-PEG5K-SH	JKA7002-1G
4arm-PEG5K-Succinimidyl Carboxymethyl Ester	JKA7014-1G
Average M_n 10,000	
4arm-PEG10K	JKP2003R-1G
4arm-PEG10K-Acrylate	JKA7068-1G
4arm-PEG10K-COOH	JKA7027-1G
4arm-PEG10K-Glutaric Acid pentaerythritol core	JKA7164-1G
4arm-PEG10K-Maleimide	JKA7018-1G
4arm-PEG10K-NH2 pentaerythritol core	JKA7011-1G
4-arm Poly(ethylene glycol) norbornene terminated	808474-1G
Average M_n 10,000	
4arm-PEG10K-SH pentaerythritol core	JKA7008-1G
4arm-PEG10K-Succinimidyl Carboxymethyl Ester	JKA7015-1G
4arm-PEG10K-Succinimidyl Carboxymethyl Glutaramide	JKA7110-1G
4arm-PEG10K-Succinimidyl Glutarate pentaerythritol core	JKA7031-1G
4arm-PEG10K-Succinimidyl Succinate pentaerythritol core	JKA7006-1G
4arm-PEG10K-Vinylsulfone	JKA7005-1G
4arm-PEG10K 2arm-OH 2arm-COOH	JKA7048-500MG
4arm-PEG10K 2arm-OH 2arm-NH2 HCl Salt	JKA7077-500MG
4arm-PEG10K 3arm-OH 1arm-COOH	JKA7047-1G
4arm-PEG10K 3arm-OH 1arm-NH2 HCl Salt	JKA7081-500MG
Average M_n 20,000	
4arm-PEG20K-Acrylate	JKA7034-1G
4arm-PEG20K-COOH	JKA7028-1G
4arm-PEG20K-Isocyanate	JKA7111-1G
4arm-PEG20K-Maleimide	JKA7029-1G
4arm-PEG20K-NH2 HCl Salt	JKA7026-1G
4-arm Poly(ethylene glycol) norbornene terminated	808466-1G
4arm-PEG20K-SH	JKA7039-1G
4arm-PEG20K-Succinimidyl Carboxymethyl Ester	JKA7038-1G
4arm-PEG20K-Succinimidyl Carboxymethyl Glutaramide	JKA7013-1G
4arm-PEG20K-Succinimidyl Glutarate	JKA7010-1G
4arm-PEG20K-Succinimidyl Succinate	JKA7030-1G
4arm-PEG20K-Vinylsulfone	JKA7025-1G
Average M_n 40,000	
4arm-PEG40K-COOH	JKA7066-1G
4arm-PEG40K-Maleimide	JKA7067-1G
4arm-PEG40K-NH2 HCl Salt	JKA7024-1G
4arm-PEG40K-Succinimidyl Carboxymethyl Ester	JKA7070-1G
4arm-PEG40K-Succinimidyl Glutarate	JKA7017-1G
4arm-PEG40K-Succinimidyl Succinate	JKA7069-1G

8arm PEGs

| Name	Prod. No.
Average M_n 10,000	
8arm-PEG10K-Acrylate, tripentaerythritol core	JKA10021-1G
8arm-PEG10K-COOH, hexaglycerol core	JKA8016-1G
8arm-PEG10K-COOH, tripentaerythritol core	JKA10004-1G
8arm-PEG10K-Maleimide hexaglycerol core	JKA8027-1G
8arm-PEG10K-Maleimide tripentaerythritol core	JKA10018-1G
8arm-PEG10K-NH2, hexaglycerol core HCl Salt	JKA8008-1G
8arm-PEG10K-NH2, tripentaerythritol core HCl Salt	JKA10001-1G
8arm-PEG10K-SH hexaglycerol core	JKA8004-1G
8arm-PEG10K-SH, tripentaerythritol core	JKA10022-1G
8arm-PEG10K-Succinimidyl Glutarate tripentaerythritol core	JKA10010-1G
8arm-PEG10K-Succinimidyl Succinate tripentaerythritol core	JKA10007-1G
8arm-PEG10K-Vinylsulfone, tripentaerythritol core	JKA10033-1G
8arm-PEG10K 7arm-OH, 1arm-COOH, tripentaerythritol core	JKA10041-500MG
Average M_n 15,000	
8arm-PEG15K-Succinimidyl Glutarate tripentaerythritol core	JKA10011-1G
8arm-PEG15K-Succinimidyl Succinate tripentaerythritol core	JKA10024-1G
Average M_n 20,000	
8arm-PEG20K-Acrylate tripentaerythritol core	JKA10016-1G
8arm-PEG20K-Acrylate, hexaglycerol core	JKA8005-1G
8arm-PEG20K-COOH hexaglycerol core	JKA8017-1G
8arm-PEG20K-COOH, tripentaerythritol core	JKA10005-1G
8arm-PEG20K-Maleimide hexaglycerol core	JKA8028-1G
8arm-PEG20K-Maleimide tripentaerythritol core	JKA10019-1G
8arm-PEG20K-NH2, hexaglycerol core HCl Salt	JKA8009-1G
8arm-PEG20K-NH2, tripentaerythritol core HCl Salt	JKA10002-1G
8arm-PEG20K-Norbornene, tripentaerythritol core	JKA10037-1G
8arm-PEG20K-SH hexaglycerol core	JKA8007-1G
8arm-PEG20K-SH, tripentaerythritol core	JKA10023-1G
8arm-PEG20K-Succinimidyl Glutarate tripentaerythritol core	JKA10012-1G
8arm-PEG20K-Succinimidyl Succinate tripentaerythritol core	JKA10008-1G
8arm-PEG20K-Vinylsulfone, tripentaerythritol core	JKA10034-1G
8arm-PEG20K 7arm-OH, 1arm-COOH, tripentaerythritol core	JKA10039-500MG
Average M_n 40,000	
8arm-PEG40K-COOH hexaglycerol core	JKA8018-1G
8arm-PEG40K-Maleimide hexaglycerol core	JKA8029-1G
8arm-PEG40K-NH2 HCl Salt, hexaglycerol core	JKA8012-1G

Y-shape PEGs

Name	Prod. No.
Average M_n 40,000	
Y-PEG40K-Acetaldehyde	JKA0003-1G
Y-PEG40K-COOH	JKA0019-1G
Y-PEG40K-MAL	JKA0002-1G
Y-PEG40K-NH2	JKA0010-1G
Y-PEG40K-NHS	JKA0001-1G
Y-PEG40K-Propionaldehyde	JKA0017-1G

Block PEGs

Name	Prod. No.
4arm-PEG2500-PCL2500	JKA9012-1G
4arm-PEG2500-PLA3500	JKA9013-1G

ALDRICH®
Materials Science

TRANSLATING
POLYMER SCIENCE
FOR DRUG DELIVERY
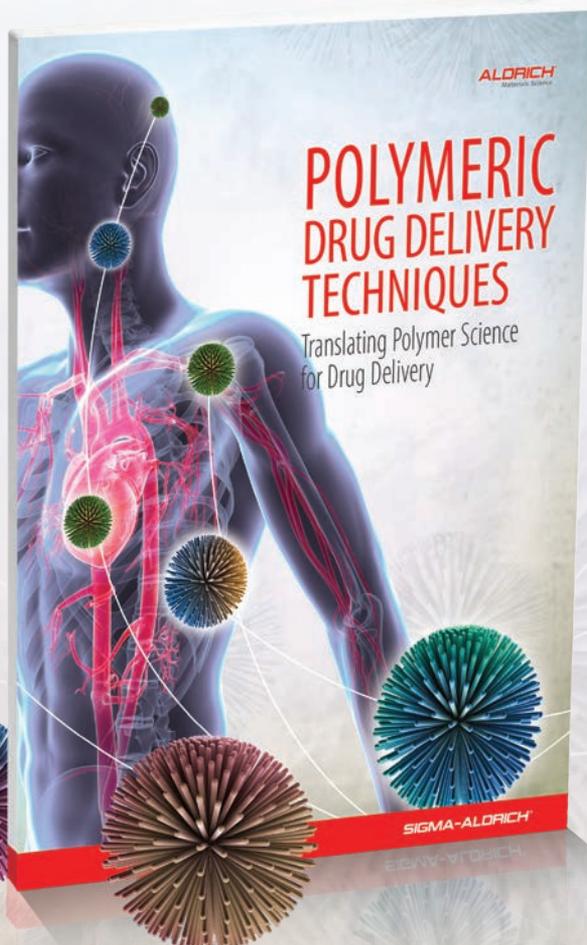
A guide to drug delivery solutions using polymers for controlled release, targeted drug delivery and solubility enhancement.

- Step-by-step methods written by drug delivery experts highlighting polymer-based methods to solve the most important drug delivery challenges
- Solutions for:
  - Small molecules
  - Nucleic acids
  - Proteins
- Key technologies:
  - Drug conjugation and PEGylation
  - Biodegradable nanoparticles and micelles
  - RAFT polymeric carriers for ADCs
  - Dendrons
  - Responsive drug delivery systems
  - Polymers for oligonucleotide delivery

Request your copy online at
aldrich.com/ddtechnique

SEI
84696-517920
1106

SIGMA-ALDRICH®